Design of a small antenna for indoor electronic monitoring

Dissertation submitted for the degree
Master of Engineering in Computer and Electronic
at the Potchefstroom campus of the North-West University

C.F. Thom

20082770

Supervisor: Prof. J.E.W. Holm
Co-supervisor: Mr. H. Marais
December 2011

Declaration

I, Carl Friedrich Thom hereby declare that the thesis entitled "Design of a small antenna for indoor electronic monitoring" is my own original work and has not already been submitted to any other university or institution for examination.

C.F. Thom

Student number: 20082770

Signed on the 13th day of December 2011 at Potchefstroom.

Acknowledgements

Thank you to my Lord and Saviour, without whom none of this is possible.

For my mom and dad, thank you for your love and support through the good times and the bad.

To Jeanine, thank you for all your support and love. I couldn't have done this without you. Love always.

Thank you to Prof. Holm for sharing his expertise and knowledge with me.

To Henri, thank you for all of the support, encouragement and advice throughout this process.

Thank you to Mrs. Louise, Mrs. Vanda and Mrs. Riana for all of the help you gave me to navigate the University administration system.

Thank you Rossouw, for the advice, components and tools you gave me.

Thank you to everyone for evenings spent with coffee in hand.

Abstract

Keywords: *Antenna, Electronic monitoring, Simulation*

The objective of this project is to design an antenna for use in the electronic monitoring of persons convicted of non-violent crimes. If implemented, electronic monitoring will lighten the load on the South African prison system. Electronic monitoring makes use of an electronic tether connected to the person being monitored. This led to specific performance requirements and size constraints being placed on the antenna. The antenna should be physically small while still being able to perform as specified. It is also necessary to test the design with various frequencies, to determine the best possible frequency to use.

It was decided to use a Transformer Coupled Loop (TCL) antenna, after various designs were considered. The TCL antenna can be used in various configurations, with some of these configurations being simulated to determine the best antenna structure to use. After various antenna structures were discarded, a specific antenna structure emerged as a possible solution, which was then optimised to deliver the best possible performance.

The optimised antenna model was constructed to test the antenna performance. The receiving antenna was a directional Log-Periodic Dipole Antenna (LPDA), connected to a spectrum analyser. Tests were conducted in an open-field environment to minimise the effect of reflections. The azimuth- and elevation radiation patterns for the antenna could be compared to the simulated results. The same tests were performed with the antenna attached to a saline solution bag, simulating the effects of the human body on the antenna performance.

The radiation patterns obtained from the measured results proved to be similar to the simulated results for both frequencies tested. When making use of the human analogue, the radiation pattern tended to be more omnidirectional in both the azimuth- and elevation planes. These results are ideal, since omnidirectional communication by the tethering device is required by a security application. The primary objective was achieved, together with the secondary objectives of comparing different frequencies.

Opsomming

Sleutel woorde: *Antenna, Elektroniese monitering, Simulasie*

Die hoofdoelwit is die ontwerp van 'n antenna wat geskik sal wees vir gebruik in 'n elektroniese monitering stelsel. Elektroniese monitering kan gebruik word om geweldlose misdadigers uit die gevangenis te haal. Deur dit te doen kan die las op die Suid-Afrikaanse gevangenisstelsel verlaag word. Daar is sekere vereistes geplaas op die grootte van die antenna. Dit is ook belangrik om die antenna te toets deur gebruik te maak van verskillende frekwensies om die beste frekwensie se bepaal.

Nadat die maksimum afmetings wat die antenna mag beslaan vasgestel is, is daar na verskeie tipes moontlike antennas gekyk. Daar is besluit om die Transformator-gekoppelde Lus-antenna te gebruik omdat daar verskeie konfigurasies van hierdie antenna is. Dit het gelei daartoe dat 'n beperkte hoeveelheid antenna konfigurasies gesimuleer word. 'n Struktuur is gevind wat aan al die vereistes voldoen, waarna dit geoptimeer is om die beste moontlike werkverrigting te lewer.

Die geoptimeerde antenna is vervaardig en daar is gebruik gemaak van 'n bestaande versender. 'n Hoogs direksionele, "Log-Periodic Dipole Antenna (LPDA)", is gebruik as ontvangsantenna en is gekoppel aan 'n spektrumanaliseerder. Die toetsing van die antenna is gedoen in 'n buitelug omgewing om die effekte van refleksies te minimaliseer. Die asimut- en elevasiestralingspatrone kon saamgestel word om vergelyk te word met die simulasieresultate. Siende dat die resultate mag verander indien die antenna na aan die menslike liggaam geplaas word, is die toetse weer gedoen met die antenna gebind aan 'n soutoplossing, wat die invloed van die mens op antenna werkverrigting weergee.

Die gemete stralingspatrone is soortgelyk aan dié van die simulasies vir beide die frekwensies wat gebruik is. Met die gebruik van die soutoplossing, is gevind dat die stralingspatroon meer omni-direksioneel is vir beide die asimut en elevasie vlakke. Dit kan beskou word as uitstekende resultate, aangesien 'n sekuriteitstelsel kommunikasie in alle rigtings wil hê. Die hoofdoelwit is dus bereik tesame met die sekondêre doelwit om verskillende frekwensies met mekaar te vergelyk.

Contents

List of Figures

List of Acronyms

BEM Boundary Element Method

DCS Department of Correctional Services

EM Electromagnetic

ETSI European Telecommunications Standards Institute

FCC Federal Communications Commission

FDTD Finite-Difference Time-Domain

FEM Finite Element Method

GFSK Gaussian Frequency Shift Keying

GPS Global Positioning System

GSM Global System for Mobile Communications

HART Highway Addressable Remote Transducer

HF High Frequency

HFSS High Frequency Structure Simulator

ICASA Independent Communications Authority of South Africa

IP Internet Protocol

ISM Industrial, Scientific and Medical

ITU-R International Telecommunications Union Radiocommunication Sector

LHC Left-Hand Circular

LHE Left-Hand Elliptical

LoS Line-of-Sight

ML Magnetic Loop

MoM Method of Moments

OID Offender Identification Device

PAN Personal Area Network

PCB Printed Circuit Board

PDE Partial Differential Equations

PDF Probability Density Function

PSTN Public Switched Telephone Network

PVC Polyvinyl Chloride

RF Radio Frequency

RFID Radio Frequency Identification

RHC Right-Hand Circular

RHE Right-Hand Elliptical

SAPS South African Police Service

SNR Signal-to-Noise Ratio

SoC System-on-Chip

SRD Short Range Wireless Device

TCL Transformer Coupled Loop

List of Symbols

c	Speed of light
λ	Wavelength
f	Frequency
f_c	Carrier Frequency
f_e	Envelope Frequency
θ	Angle
n	Index of Refraction
P	Power
P_t	Power Transmitted
P_r	Power Received
G_t	Gain of the Transmitting Antenna
G_r	Gain of the Receiving Antenna
R	Distance in m
L_p	Path Loss
L_{fs}	Free-space Path Loss
h	Base Station Height in m
d	Distance in km
n	Antenna Efficiency
l	Antenna Perimeter
A	Enclosed Area of Antenna

Chapter 1

Introduction

This chapter will outline the primary research objective together with any additional research objectives.

1.1 Background

1.1.1 Prison overcrowding in South Africa

The South African prison system is experiencing severe overcrowding at the moment [1]. South African prisons are at 137.25% of their capacity. The number of trial-awaiting detainees numbered 49695 at the end of the 2010/2011 financial year. This accounts for roughly 53% of the available capacity of the prisons in South Africa. It is estimated by the Department of Correctional Services (DCS) that the cost for incarcerating these persons is in the region of R120 per person per day [1]. It is possible to save a large amount of money by making use of alternative methods to detain the trial awaiting persons. An electronic monitoring system is a possible solution that may address the capacity shortages experienced by modern prison systems.

Electronic monitoring can address the capacity problem in several ways. A convicted white-collar criminal (a criminal committing non-violent crimes like fraud, identity theft, etc.) may be fitted with one of these devices and placed under house-arrest, thereby removing the burden of sustaining them from the state. Another way in which electronic monitoring can contribute to the reduction of prison overcrowding is by placing criminals convicted of non-violent crimes under house-arrest until they have finished serving their sentence. If a convicted felon is released on parole, he may also be fitted with an electronic monitoring system. To ensure the success of such an electronic monitoring system, it should be operated in a partnership between the DCS as well as the South African Police Service (SAPS).

1.1.2 Electronic monitoring

1.1.2.1 Overview of electronic monitoring

Electronic monitoring systems, or electronic tagging as it is sometimes known, is used to monitor persons or vehicles [2]. It should be understood that the term "Monitoring", refers to monitoring of the whereabouts of the offender. The persons being monitored are usually convicted felons. Electronic monitoring works by attaching a device (hereafter referred to as a tether) to the ankle of the person being monitored (as depicted in Figure 1.1). The tether is monitored by a central monitoring authority to ascertain the whereabouts of the person being monitored.

1.1.2.2 Operating modes

The tether communicates, either directly or indirectly, with the monitoring authority responsible for monitoring the felon's whereabouts. When making use of direct communication, the tether is equipped with a Global Positioning System (GPS) receiver and communicates via a cellular network, typically Global System for Mobile Communications (GSM). When operating in the indirect communication mode, the

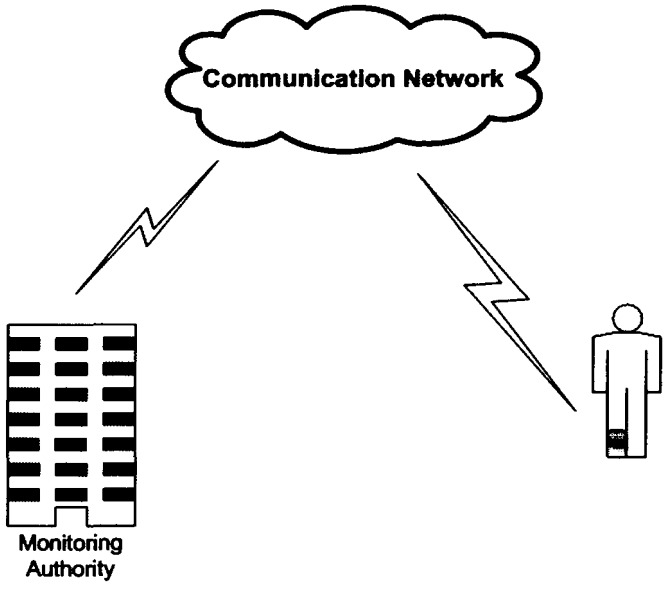

Figure 1.1: Conceptual model of an electronic monitoring system

tether makes use of short-range wireless communication to communicate with a base station.The tether is limited to a specific area around the base station due to the limitations of Short Range Wireless Devices (SRDs). The base station communicates with the monitoring authority by means of GSM, Public Switched Telephone Network (PSTN) or Internet Protocol (IP) infrastructure.

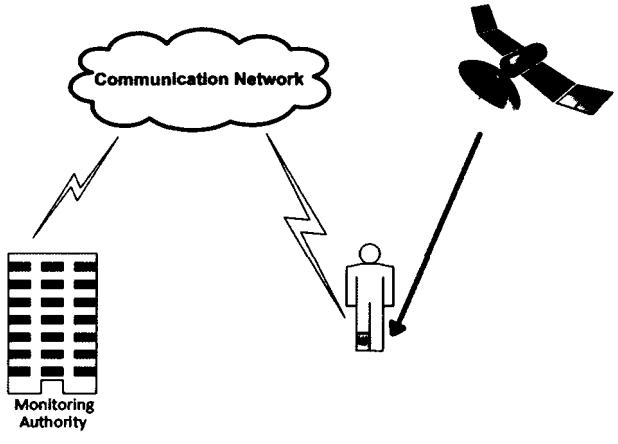

Figure 1.2: Direct communication mode

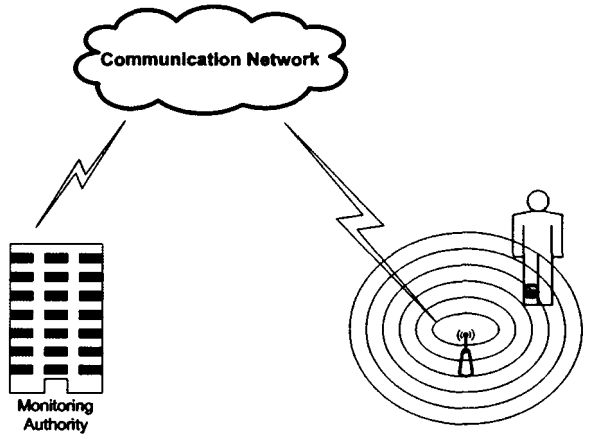

Figure 1.3: Indirect communication mode

Figure 1.2 depicts an electronic monitoring system's direct communication mode in

which the tether receives GPS coordinates and transmits these coordinates to the monitoring authority, while Figure 1.3 shows the indirect mode for the electronic monitoring system.

Operating in the direct communication mode, the tether only communicates its GPS coordinates (and thus the coordinates of the felon) to the monitoring authority. Communication with the GPS satellites are strictly one-way. Before being fitted with the tethering device and set under house-arrest, the authority responsible for monitoring the location of the offender needs to set a prescribed area where the offender may move freely. The monitoring authority is then responsible for determining if the offender has left this prescribed area or if the felon is tampering with the tether. These devices are limited in their range of operation only by the availability of a cellular signal, as this is the main form of communication. The main drawback of the direct communication operating mode is the power consumption of the tethering device. Since it needs to receive regular updates from the GPS, as well as send this information via the cellular network to the monitoring authority. All of this wireless activity puts the battery needed under serious strain, thereby leading to regular battery changes.

For the indirect communication scenario, the base station will alert the monitoring authority if the offender leaves the prescribed area, which falls within the base station's reception area. The size of the reception area is determined by various factors, including the transmitted power of the tether, the gain of the antennas used in the tether and the receiver, as well as any amplification used in the receiving device. In an indoor environment, the range is severely limited by this environment.

1.2 Research objectives

From the previous section, the operating modes were explained in relative detail. It is important analyse the system and from there to deduce what the most important problem is to solve. To simplify the problem, it is important to place certain limitations on the system. Due to some of the complexities involved, the direct communication

mode is not considered.

If only the indirect communication mode is considered, the following simplifying assumptions can be made:

- Transmitter and receiver hardware are freely available as off-the-shelf components;
- The receiver antenna can be purchased.

In Figure 1.4 an abstraction of the electronic monitoring communication system is shown.

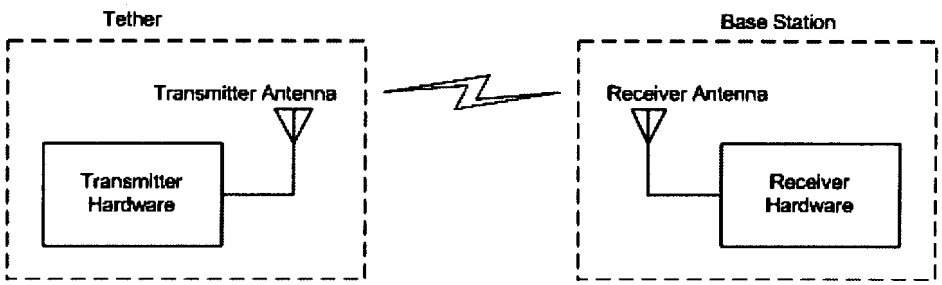

Figure 1.4: Schematic representation of the local subsystem configuration

When comparing the assumptions with Figure 1.4, only the receiving antenna and wireless communication channel remain. The most important aspect of these two is probably the transmitting antenna.

By taking the preceding section into account, the research objective becomes

THE DEVELOPMENT OF A PHYSICALLY SMALL ANTENNA FOR INDOOR ELECTRONIC MONITORING

Since the antenna forms part of the tether (hereafter referred to as the Offender Identification Device (OID)) it is subject to certain constraints.

The main constraints are:

- **Size:** Since the OID is connected to the ankle of the offender being monitored, it needs to be small and compact. The antenna therefore needs to fit inside the same enclosure as the electronics and battery of the OID;
- **Reliability of Communication:** Since electronic monitoring is a security application, it is necessary for the OID to be able to communicate reliably in different conditions and in various orientations relative to the base station;

As the OID makes use of wireless communication, different wireless communication technologies should be investigated before committing to a specific solution. To this end some secondary research objectives are defined.

Secondary research objectives include:

- Investigating the suitability of various communication technologies;
- The selection of the optimal communication frequency. This is dependent on the selected wireless technology chosen for use in the electronic monitoring system.

1.3 Dissertation overview

The literature survey acts as a reference for the information required to successfully design and implement a specific antenna design.

In the methodology chapter, the methods used to design, construct and test the antenna are discussed together with the design decisions.

In the design and simulation chapter, the design of the antenna is done according to all of the required specifications, after which it is simulated in order to evaluate the design before implementing it. The results are analysed and discussed before reaching the implementation phase.

In the physical implementation and results chapter, the construction of the antenna is discussed together with the experimental set up. The results of the tests performed are also discussed in detail.

Conclusions are made regarding the design process, the simulation and design of the antenna as well as the performance of the implemented antenna in the conclusions and recommendations chapter. Furthermore some recommendations are made for any future work to be done on this project.

Chapter 2

Literature survey

This chapter provides the theoretical background necessary to understand antennas and their design. Various communications protocols are also discussed in order for a decision to be made regarding which is the best one to use.

2.1 Introduction

Since this study is only concerned with the design of the antenna to be used in the tethering device, the other design considerations will not be discussed. This includes the electronic design together with power supply considerations. Another important very important design aspect is the anti-tampering methods employed in this device. These factors are important, but irrelevant to this research.

This chapter provides some background for the antenna design. The chapter will commence by providing information on Radio Frequency (RF) communication and Electromagnetic (EM) theory on which operation of antennas are based. Antenna parameters will also be discussed in order to gain a better understanding of antennas and

their operation in general.

Different antennas and wireless solutions will also be discussed in order to select the best antenna structure and frequency to use.

2.2 Communication systems

2.2.1 General communication system

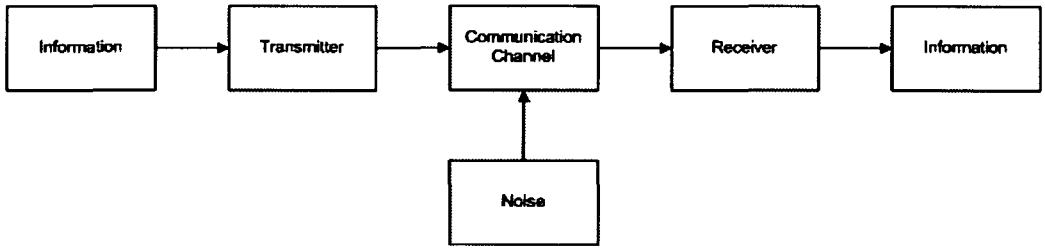

Figure 2.1: General communication system [3]

Figure 2.1 is a representation of a general communication system which consists of information, a transmitter, a communication channel with noise, a receiver and the received information. An information signal acts as input to the transmitter which transmits the information signal to a receiver via a communication channel. The transmitter is responsible for converting the information signal into the correct form for transmission over the communications channel. The communications channel may be wire, fibre optic cables or even free-space for radio transmission. Every communications channel is susceptible to noise, therefore an external noise source is also included in Figure 2.1 as indicated. The receiver is responsible for retrieving the information signal from the noisy communication channel, with the original information signal being the output of the communication system [3].

Communication can be either simplex or duplex in nature. Simplex communication allows communication only in one direction, from a transmitter to a single receiver, or multiple receivers. This is the method used by Television (TV)- and radio broadcast system. Duplex communication can be either half-duplex or full-duplex. Half-duplex allows communication in both directions, but only in one direction at a time. A general example of a half-duplex communication system is two-way radio's (including amateur radio). Full-duplex allows communication in both directions at the same time. A PSTN is an example of a full-duplex communication system. The main drawback of full-duplex communication is that two different channels needs to be used to achieve this, thereby increasing the complexity of the system as well as increasing the overhead required to operate such a system [3] [4].

2.2.2 Wireless communication

Figure 2.2: Wireless communication system - Adapted from [3]

Wireless systems generally make use of an RF link, though optical wireless systems such as infra-red may also be used, especially in general appliances [3], [4], [5] . Optical solutions are used for extreme short-range communication and are also highly directional. The frequencies used for RF communication are much higher than the frequencies generated by human speech or data. It is therefore necessary to superimpose the information signal onto a carrier signal. This is done by the transmitter by means of a process called modulation. At the same time the receiver performs the inverse process while retrieving the information, called demodulation.

2.2.3 Radio frequency communication system

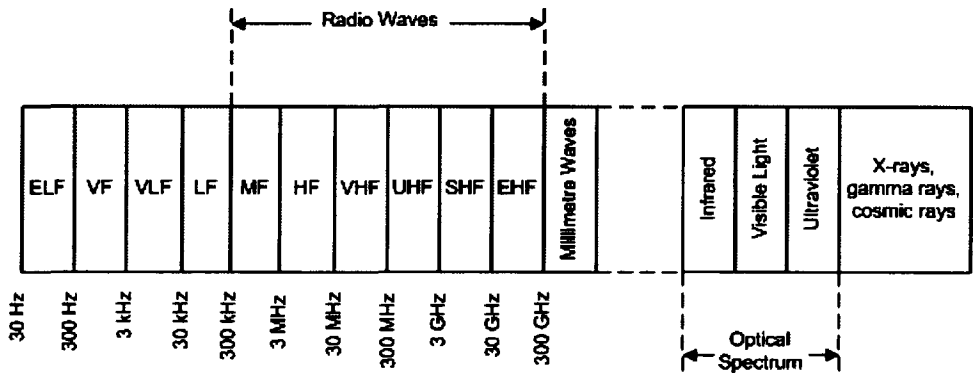

Figure 2.3: Electromagnetic spectrum [4]

From the EM spectrum shown in Figure 2.3, it can be seen that the radio frequency spectrum for use in communication systems covers the range from medium frequencies to extremely high frequencies. The optical spectrum forms part of the EM spectrum and is therefore also shown in Figure 2.3, but it does not fall within the range of frequencies used for radio communication.

2.2.3.1 High frequency

High Frequency (HF) covers the band from 3 MHz to 30 MHz and is mainly used by amateur radio enthusiasts. Because of the relatively low frequency, it allows long-range communication. Citizens band radio, which allows short-range communication between persons for private and commercial use also makes use of the HF band [4], [6].

2.2.3.2 Very-high frequency

The Very-High Frequency (VHF) range is from 30 MHz to 300 MHz and is used primarily by analogue TV broadcasts [7]. VHF has some desirable propagation characteristics that make it ideal for broadcasting. It is not readily reflected by the ionosphere and therefore the transmission range can be assumed to be Line-of-Sight (LoS). LoS is the

most direct route that a signal can travel. Atmospheric interference also does not affect VHF signals as much [4].

2.2.3.3 Ultra-high frequency

Ultra-High Frequency (UHF) ranges from 300 MHz to 3 GHz and is used for TV broadcasts. Since the higher frequency is more sensitive to atmospheric interference, UHF TV degrades faster during heavy rain or snow. The main advantage of the higher frequencies are the smaller antennas that can be used due to the shorter wavelengths [4].

2.2.4 Regulations

The International Telecommunications Union Radiocommunication Sector (ITU-R), European Telecommunications Standards Institute (ETSI) and Federal Communications Commission (FCC) are responsible for the regulation and management of radio communications. In South Africa, these duties are performed by Independent Communications Authority of South Africa (ICASA). Part of these duties includes the allocation of RF spectrum as well as the development of standards that ensure the efficient use of the limited spectrum available. The Industrial, Scientific and Medical (ISM) radio bands are a set of frequencies defined by the ITU-R for use by the industrial, scientific and medical community [8]. The frequencies defined as part of the ISM bands are given in Table 2.1. Some of these frequencies are location specific, like the 915 MHz frequency which is used in the Americas and Greenland. Other frequencies may be allocated as unlicensed bands, but does not form part of the ISM bands.

When developing a product based on a wireless system, the frequency at which it operates is important. Ideally, it is good practice to make use of part of the RF spectrum that is license free or part of the ISM bands. This is especially important for commercial applications where high volumes would incur substantial licensing fees. The two most viable frequencies that may be used in South Africa, 434 MHz and 868 MHz, are set in

Table 2.1: ISM band frequencies [8]

Frequency Range		
Lower Frequency (MHz)	Upper Frequency (MHz)	Centre Frequency (MHz)
6.765	6.3795	6.780
13.553	13.567	13.560
26.957	27.283	27.120
40.660	40.7	40.680
433.050	434.790	433.92
902	928	915
2400	2500	2450
5725	5875	5800
24000	24250	24125
61000	61500	61250
122000	123000	122500
244000	246000	245000

amateur radio bands and for general use by SRDs.

2.3 Radio frequency communication

2.3.1 Introduction

2.3.1.1 Maxwell and electromagnetic waves

The work done by James Clerk Maxwell is fundamental to our understanding of EM waves and the way in which these waves propagate through space [9]. The equations known as Maxwell's Equations predict the propagation of EM waves away from a time-varying source. This does not only apply to radio waves, but to any form of EM waves, including ultraviolet light, the visible spectrum and x-rays. Maxwell's equations provide the relationship between the electric field vector **E** and the magnetic field vector **H** respectively. As vectors, **E** and **H** have both magnitude and direction and are always perpendicular to one another, forming a Transverse Electromagnetic (TEM) wave [10].

2.3.1.2 Plane waves

The uniform phase front radiated by a finite radiator becomes planer in a small region and **E** and **H** lies in a plane, thus the name plane wave. By using these plane waves and a method called the Uniform Plane Wave (UPW) to solve Maxwell's equations for radiating problems, the solutions become easier [11]. Figure 2.4 illustrates plane waves propagating in the z-direction.

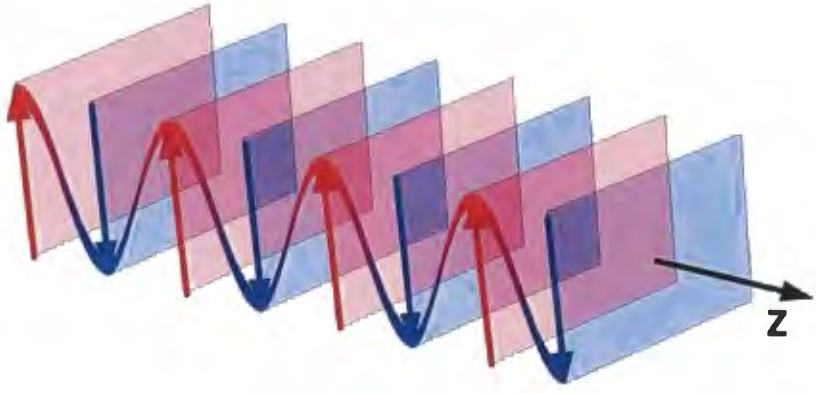

Figure 2.4: Plane waves

2.3.1.3 Polarisation of electromagnetic waves

The polarisation of a plane wave can be seen when observing **E** from a fixed observation point. If the plane wave moves in the +z-direction of the three-dimensional space XYZ, then the electric field is polarised in the x-y plane and described in terms of two perpendicular components. There are three basic types of polarisation: linear-, circular- and elliptical polarisation [11], [10], [12].

Linear polarisation: If the electric field moves linearly along the same axis, the plane wave is said to be linearly polarised. This can be either vertical (Figure 2.5) or horizontal (Figure 2.6). The magnetic field is perpendicular to the electric field at all times [11].

Circular polarisation: If the length of the electric field vector remains constant, but it rotates in a circular path, it is said that the plane wave has circular polarisation.

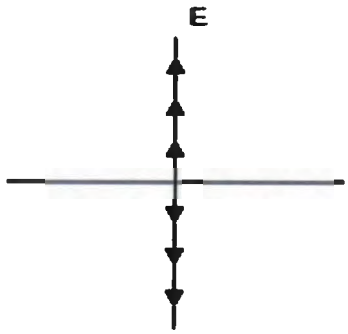

Figure 2.5: Vertical linear polarisation

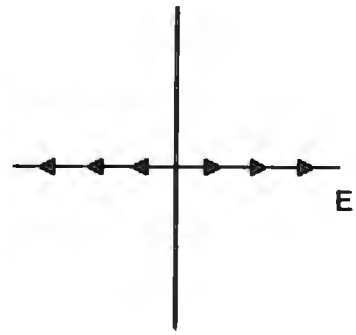

Figure 2.6: Horizontal linear polarisation

This can either be Left-Hand Circular (LHC) polarisation (Figure 2.7) or Right-Hand Circular (RHC) polarisation (Figure 2.8) [11]. This can be visualised by assuming that a circular polarised wave is heading in the direction of an observer. If the plane wave rotates clockwise, it is said to be LHC polarised, otherwise it is RHC polarised.

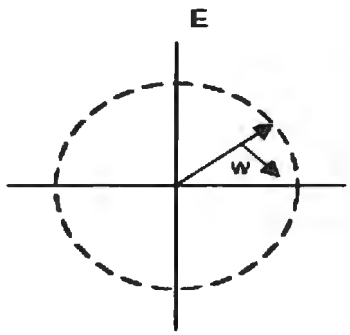

Figure 2.7: LHC polarisation

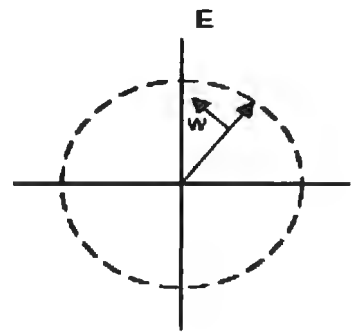

Figure 2.8: RHC polarisation

Elliptical polarisation: When the field vector rotates in a circular path and its length varies, the wave is said to have elliptical polarisation. The direction in which it rotates is also called the Left-Hand Elliptical (LHE) and Right-Hand Elliptical (RHE) polarisation. This is a special case of circular polarisation [11].

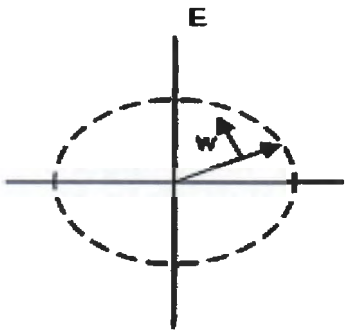

Figure 2.9: LHE polarisation

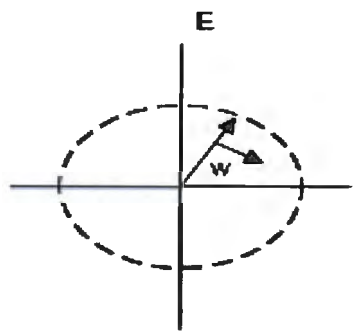

Figure 2.10: RHE polarisation

2.3.1.4 Propagation of electromagnetic waves

The Maxwell equations state that a time-varying current generates a circulating and time-varying magnetic field, **H**. Through Faraday's Law, this time varying magnetic field generates a circulating and time-varying electric field, **E**. The electric field then generates a magnetic field through Ampere's Law and this continues ad infinitum [13]. Since **E** and **H** are perpendicular, when visualising the way in which an EM wave propagates through space, it looks like a chain where each link is either a circulating magnetic field, or a circulating electric field.

The direction of propagation of a plane wave with a fixed frequency is given by the Poynting vector, which points in the direction of propagation while its magnitude oscillates [11], [10]. The Poynting vector, **S**, has units of W/m^2 and provides the power density which is normal to **S**.

2.3.2 Propagation effects

As a radio wave propagates through space, it will encounter many different objects including buildings, auto mobiles, vegetation, etc. All of these objects will affect the wave. A simplifying assumption can be made that radio waves act in a similar manner to light waves. The influence of various objects on radio waves is then easier to understand. Light can be reflected, refracted, diffracted and focused. Just as a lens

focuses a light, an antenna focuses radio waves to propagate in a specific direction. These propagation effects will now be discussed in greater detail.

2.3.2.1 Reflection

As light falls on a reflective surface, it is reflected back from this surface [4]. The angle of reflection is the same as the angle of incidence. In the same way any conducting surface acts as a reflective surface for radio waves. This is especially true if the object is half the length of the wave for the particular frequency. Buildings, auto mobiles, planes, trains and power lines all cause reflections of the propagating wave. The better conductor a the reflector is, the better it reflects the wave. As there are no perfect conductors, a portion of the energy of the wave will be absorbed by the reflective surface. It should also be noted that the phase of the reflected wave is 180° out of phase of the incident wave [4]. The reflection of an incident wave is illustrated in Figure 2.11.

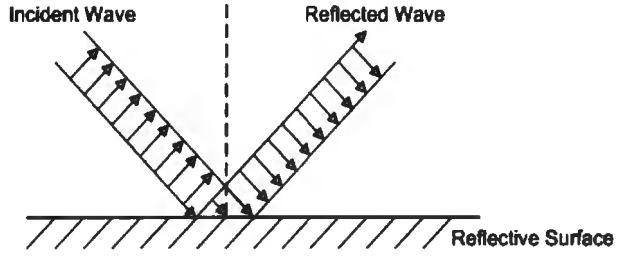

Figure 2.11: Reflection [4]

2.3.2.2 Refraction

The medium through which the wave propagates can cause the wave to bend [4]. This is called refraction. The amount of refraction depends on the index of refraction for the medium through which the wave is travelling. Since radio waves propagate at almost the same speed through air as through a vacuum, it can be said that air has an index of refraction close to 1. Another medium will have an index of refraction higher than 1 [4]. Refraction is illustrated in Figure 2.12.

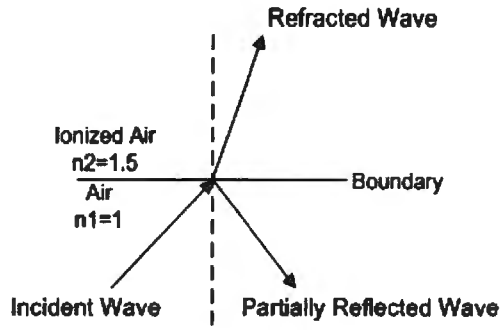

Figure 2.12: Refraction [4]

The relationship between the indices and angles of refractions is given by Snell's Law in Equation 2.1 [4]:

$$n_1 sin\theta_1 = n_2 sin\theta_2 \tag{2.1}$$

2.3.2.3 Diffraction

As radio waves travel through space, it is liable to be blocked by objects in its path. When the object blocks part of the signal, it creates a shadow zone where a receiver in the shadow zone will not be able to receive the complete signal. Due to the bending of the wave around the object, also called diffraction, some of the signal might still reach the receiver [4].

2.3.2.4 Multipath

Multipath propagation is the result of multiple radio signals, travelling from the antenna of a transmitter to the antenna of a receiver, each reaching the receiver antenna by slightly different paths due to reflections from objects encountered in the environment, such as ground reflections. This can lead to constructive or destructive interference as well as phase shifts at the receiving antenna [4], [3].

A phase shift occurs because the reflected signals arrive at the receiver at a later time than the signal travelling the LoS route. Radio waves that are 180° out of phase cancel out one another. This is what is referred to as destructive interference. Constructive interference is when the radio waves are in phase and they therefore increase in magnitude. Figure 2.13 illustrates a simplified scenario for multipath propagation. In reality there are a large number of waves reflected from objects in the environment [4], [3].

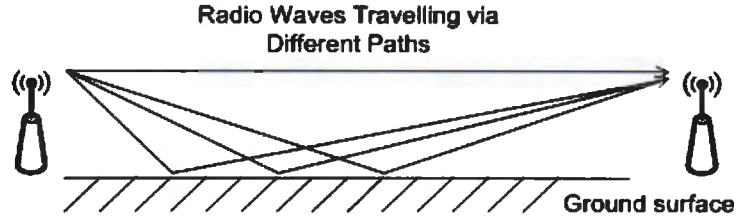

Figure 2.13: Multipath propagation

Fading: Another effect of radio wave propagation is called fading. Fading refers to the variation in received signal amplitude due to the effects of multipath propagation, reflection, refraction, diffraction and scattering.

Shadow fading: This usually occurs when the transceivers are moving. If the transceivers move behind a building, the fading that occurs is called shadow fading. Atmospheric effects, such as rain or snow may also cause shadow fading by moving between the transmitter and the receiver. This is especially pronounced at higher frequencies where the size of the snow flakes and water droplets are similar to the wavelength of the radio wave [4], [5].

2.3.3 Channel models

2.3.3.1 Introduction

Channel models are mathematical representations of the way in which radio waves propagate through different channels [14]. Different channel models are for use in different environments, like free-space, urban, rural, etc., while other channel models

makes provision for the environment. A limited number of well-known and widely-used channel models are discussed.

2.3.3.2 Friis free-space model

The Friis transmission equation was derived by Harald T. Friis [15] in 1946. The equation provides a means for calculating the received power of a receiver when all other variables are known. Friis assumed that propagation takes place in free-space and therefore the Friis equation (equation 2.2) is also called the free-space equation.

$$P_r = P_t + G_r + G_t + 20log_{10}(\frac{\lambda}{4\pi R})^2 \tag{2.2}$$

P_r = Power Received;

P_t = Power Transmitted;

G_r = Gain of the Receiving Antenna;

G_t = Gain of the Transmitting Antenna.

The Friis equation is dependent on idealised conditions that are not practically realisable. For satellite communications, many of the propagation effects do not play a role or are severely diminished, thus the conditions are as ideal as possible and therefore the Friis transmission equation may be used [12]. The main aim of the Friis equation is to establish some theoretical reference.

2.3.3.3 Rayleigh fading channel

The Rayleigh fading channel makes use of the Rayleigh distribution to model the communications channel. This refers to the Rayleigh Probability Density Function (PDF), as illustrated in Figure 2.14, used to mathematically describe the variation of the received signal [4].

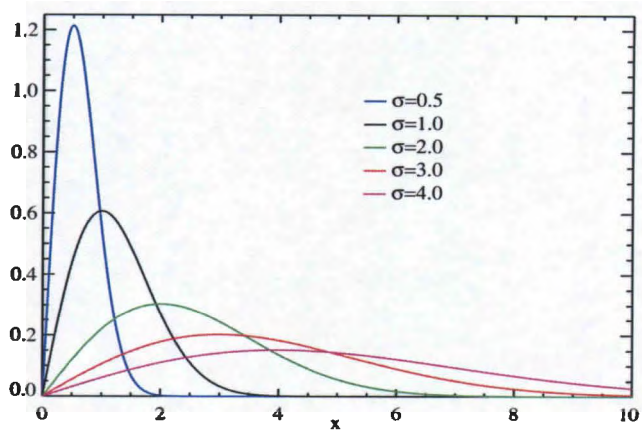

Figure 2.14: Raleigh PDF

The Rayleigh fading channel is a reasonable model and can be applied to tropospheric and ionospheric propagation [16]. The effect of a dense urban environment on radio wave propagation is also successfully modelled by a Rayleigh fading channel. It has been shown that the communications channel in Manhattan, New York closely approximates a Rayleigh fading channel [17].

2.3.3.4 Rician fading channel

A Rician fading channel is similar to the Rayleigh fading channel in that it receives a large number of reflected and scattered radio waves. The difference, however, lies therein that in a Rician fading channel a dominant LoS component is present. The Rician fading channel makes use of a Rician distribution (Figure 2.15) to mathematically model the propagation of radio waves [18], [19]. Because Rayleigh and Rician channel models are mainly used for dense urban environments, like Manhattan, it is not suited for use in the general South African environment.

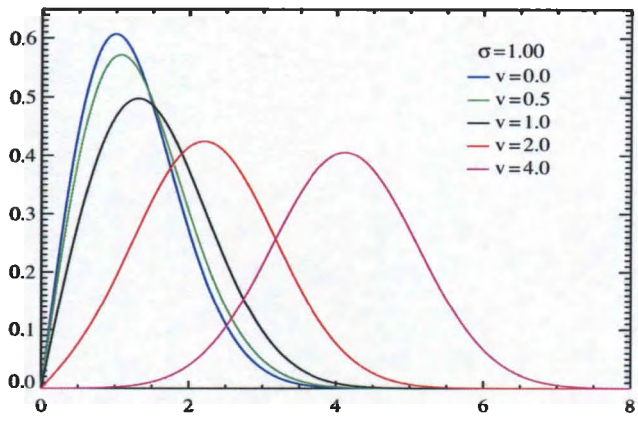

Figure 2.15: Rician PDF

2.3.3.5 Hata mobile communication model

The Hata mobile communications model [20] is used to predict the behaviour of radio waves for use by cellular systems in urban environments. It has successfully been proven to work in Manhattan, New York [17]. A simplified version of the Hata mobile communications channel model is given in equation 2.3,

$$L_p = 68.75 + 26.16log_{10}f - 13.82log_{10}h + (44.9 - 6.55log_{10}h)log_{10}d \qquad (2.3)$$

L_p = Path loss, dB;

f = Operating Frquemcy, MHz;

h = Antenna Height, m;

d = Transmission Distance, km.

It is mainly used to calculate the path loss in an urban environment, and when comparing the Hata model to the Friis results, it can be seen that free-space loss occurs faster with the Hata model than it does with the Friis model. According to the Hata model, increasing the height of the base station antenna reduces the loss experienced by the radio waves. As mentioned, Hata is used mainly for cellular devices and not intended for use by SRDs or Radio Frequency Identification (RFID). Therefore it is not a suitable channel model to use with the electronic monitoring system.

2.3.3.6 Propagation for Short-Range Devices

The model described in this section was specifically developed for use with SRDs and developed from experimental data [21]. Because it was developed from experimental data, it provides a much clearer picture of the actual path-loss experienced by SRDs. It starts by determining the isotropic path-loss, determined by using Equation 2.4.

$$PL_{ISO} = -27.55 + 20logfR \tag{2.4}$$

The general path loss can then be calculated by using Equation 2.5

$$PL = C + 10nlogR \tag{2.5}$$

C is the isotropic path-loss at 1 m and n is a factor relating to the slope of experimental data. For lossless dispersion, n = 2, while n = 4 is an approximation of indoor losses. This model is only accurate over short distances, before the phase difference reaches 180° [21].

2.4 Basic antenna theory

To better understand the objective of designing an antenna, it is necessary to understand the terminology used. This section introduces some of the more common antenna terminology.

2.4.1 Antenna

An antenna is a metallic structure that acts as a transducer to convert electric current into EM waves, and EM waves into electric current [11]. It can also be described as the device that bridges the gap between some sort of a feed, and free-space.

2.4.2 Radiation intensity

In a given direction, the power radiated per unit solid angle is called the radiation intensity, U. The solid angle is a section of the imaginary sphere surrounding the radiator, in this case an antenna [11].

2.4.3 Gain

The gain of an antenna is the ratio of the radiation intensity in a specific direction and the radiation intensity obtained if the antenna radiated the power fed into it isotropically [11]. The gain of the antenna is given in Equation 4.4.

$$G = 4\pi \frac{U}{P_{in}} \tag{2.6}$$

2.4.4 Directivity

Directivity can be seen as the ratio of the radiation intensity in a given direction from the antenna to the radiation intensity averaged over all directions [11]. The directivity of an antenna is closely related to the gain of the antenna, as the direction of maximum directivity is also the direction of maximum gain.

2.4.5 Bandwidth

The bandwidth can be defined as the range of frequencies over which the performance of the antenna conforms to some standard, with respect to a specific characteristic [11]. The bandwidth can also be defined as the ratio of upper limit frequency to lower limit frequency [3].

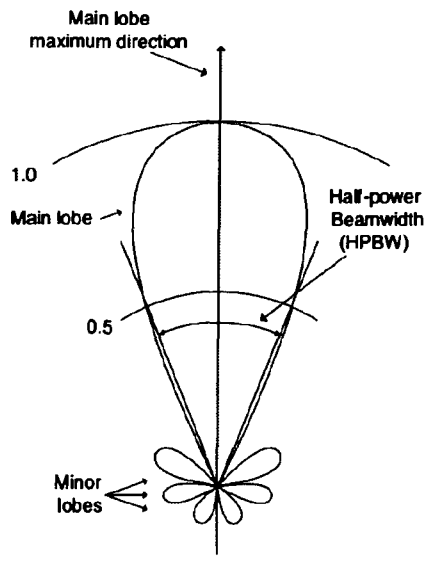

Figure 2.16: Typical antenna radiation pattern illustrating high directivity [22]

2.4.6 Resonance

At certain frequencies, called the resonant frequency of the structure, a transducer will be more efficient [11], [10]. For an antenna, this means that even electrical signals with small amplitudes are converted to EM waves with larger amplitudes if the electrical signal is at the resonant frequency. When designing an antenna, the goal is to make the structure resonate at the frequency of operation.

2.4.7 Polarisation

The polarisation of an antenna in a given direction is the polarisation of the EM wave radiated by the antenna in that direction [10]. The direction of maximum gain is to define polarisation if no direction is specified. For the best possible transmission, the transmitting and receiving antennas should have the same polarisation.

2.4.8 Diversity

Diversity refers to a scheme whereby the reliability of transmitting a message is increased [23]. This is achieved by using multiple communication channels to combat the fading and multipath effects experienced by one communications channel by using the other channels. This is due to the fact that different communications channels will experience different levels of fading and multi-path propagation effects. The receiver will receive multiple copies of the same message from different sources and therefore the message can be reconstructed.

2.4.9 Reciprocity

Antennas that do not contain non-linear and unilateral elements can be described as being a reciprocal device [11]. This means that the essential properties do not depend on whether the antenna is used as a transmitting antenna or a receiving antenna. The following properties remain the same on a reciprocal antenna:

- Antenna impedance;
- Electrical length of antenna;
- Radiation pattern;
- Directivity.

2.4.10 Field regions

The region around an antenna can be subdivided into three different regions [24]. The region closest to the antenna is called the reactive near-field region and no energy dissipation occurs in this region. The radius of this region is given by Equation 2.7:

$$R_1 = 0.62\sqrt{\frac{D^3}{\lambda}} \tag{2.7}$$

The radiating near-field region (also called the Fresnel region) is the next region and although a reactive field exists, it is dominated by the radiant fields. Equation 2.8 gives the radius of the radiating near-field region.

$$R_2 = \frac{2D^2}{\lambda} \tag{2.8}$$

Furthest from the antenna is the far-field region (or Fraunhofer region). The radiation fields are the only fields that exist in this region. The power density here is equal to the inverse square of the distance from the antenna. The various field regions are illustrated in Figure 2.17.

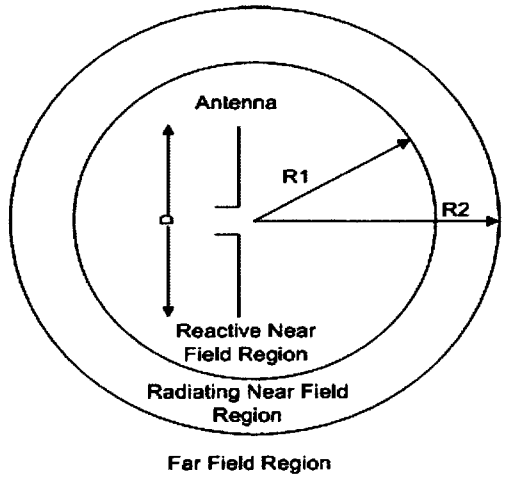

Figure 2.17: Antenna field regions [11]

2.4.11 Radiation pattern

The radiation pattern is a spatial distribution of a quantity and is used to characterise the EM field generated by the antenna. The quantity used may be the gain, the radiation intensity, directivity, and polarisation or phase power flux density. A typical

3-Dimensional gain radiation pattern is illustrated in Figure 2.18. The gain is depicted radially away from the origin of the coordinate system used, to illustrate the radiation pattern. The red region in Figure 2.18 is further from the origin of the gain plot and therefore has less gain than the yellow region (closer to the origin).

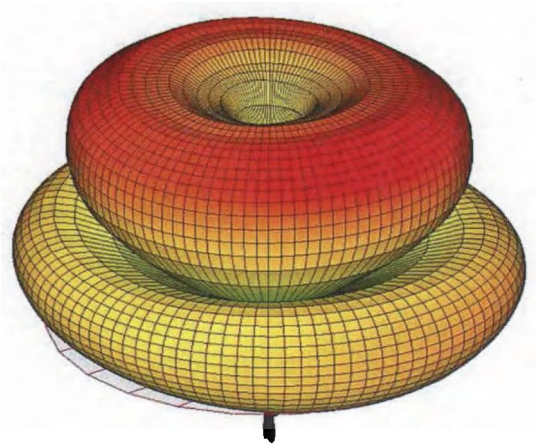

Figure 2.18: Radiation pattern of a dual-blade GSM antenna

2.4.12 Efficiency

The radiation efficiency is defined as the ratio of the total power radiated by the antenna to the total power accepted by the antenna. Efficiency can be expressed as in equation 2.9

$$\eta = \frac{P_{output}}{P_{input}} \tag{2.9}$$

2.5 Antennas

There are two basic types of antennas, electrical antennas and magnetic antennas. With electrical antennas, the **E** field is dominant in the antenna near-field (Fresnel) region. With magnetic antennas, the **H** field is dominant in the Fresnel region. In the far-field (Fraunhofer) region, the ratio of **E**/**H** is constant.

2.5.1 Size characteristics of antennas

There are certain characteristics that are common to both types of antennas, electrical and magnetic. This has to do primarily with the size of the antenna.

2.5.1.1 Small antennas

An antenna can be defined as electrically small if it can be physically bounded by a sphere with radius $\frac{\lambda}{2\pi}$ [25]. Some antennas may not necessarily be electrically small, but shows a definite size reduction in a specific plane. These types of antennas are physically constrained antennas. If an antenna does not satisfy the conditions for electrically small or physically constrained, but still manages to achieve additional performance, it can be labelled as a functionally small antenna [25], [10]. The last type of small antenna is called a physically small antenna. An antenna does not necessarily have to fall in one of the above categories to qualify as a physically small antenna. Physically small antennas have dimensions that can be regarded as small in a relative sense.

2.5.2 Effect of human proximity

Since the OID is going to be worn close to the human body, the effect of the human body on antenna performance should be considered. When looking at an antenna in close proximity to a conducting body (like the human body), the magnetic field intensity **H** is higher than the electric field intensity **E**. From Figure 2.19 it can be seen that at a frequency of 152 MHz the difference between the magnetic field intensity and the electric field intensity reaches almost 12 dB.

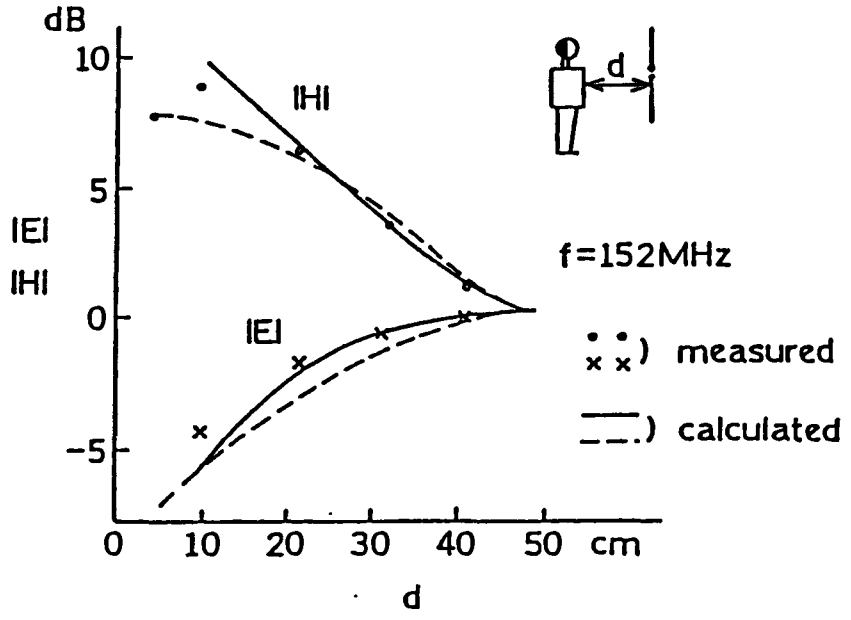

Figure 2.19: Field intensity **E** and **H** in front of a human body [25]

2.5.3 Antenna design considerations

From sections 2.5.1.1 and 2.5.2, it follows that a physically small magnetic antenna should be used for the OID. This will enable the OID to fit around the ankle of the person being monitored while still achieving the desired performance. It is therefore necessary to discuss various designs of magnetic antennas and their suitability.

2.5.4 Magnetic antennas

The first type of magnetic antenna that is discussed is the Very Small Magnetic Loop (VSML). It typically has a very low radiation resistance and therefore the efficiency is also very low. Because of this low efficiency, the VSML antenna is usually reserved for use as a receiving antenna and therefore it is not ideal for use in electronic monitoring [25]. The Signal-to-Noise Ratio (SNR) of the VSML can be improved by cooling the antenna, but this leads to a reduction in bandwidth.

The second type of antenna is the VHF/UHF Magnetic Loop. Loop antennas have been successfully implemented in hand-held devices for both the VHF and UHF bands [25], [10], [24]. The efficiency of these types of antennas can be increased by making use of ferrite materials. The Magnetic Loop (ML) antenna couples with any conductor close to it, thereby increasing the antenna efficiency even further. By placing passive components, like capacitors or inductors, in the loop, the radiation pattern can be varied. Any form of loop antenna will resonate when the perimeter of the loop is approximately one wavelength in length. From the preceding sections the combined frequency range for VHF and UHF is 30 MHz to 3 GHz. This translates to a wavelength of 10m at 30 MHz to 10cm at 3 GHz. For proper operation, the VHF frequencies are too low and therefore the antenna structure will be physically too large for use in the OID.

Another type of antenna that shows promise is the Transformer Coupled Loop (TCL) antenna. A small loop is connected to the larger loop of a ML antenna (Figure 2.20). Transformer action is achieved by the magnetic coupling between the small (primary) loop and the large (secondary) loop. A capacitor is placed in the large loop, mainly to cancel the loop inductance of the large loop. The mutual inductance of this transformer is used to transform the low loop resistance to a desired impedance. The desired value will allow for proper matching of the antenna to the transmitter, which in turn will allow the antenna to transfer the maximum amount of power. Therefore maximum performance is achieved while still retaining the small physical size of the antenna. The TCL antenna is thus selected for use in the OID [26].

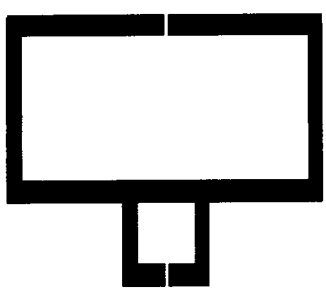

Figure 2.20: TCL antenna [26]

2.6 Wireless technologies

Various wireless technologies exists for point-to-point full-duplex communications between devices. The advantages and disadvantages of different wireless technologies will now be discussed in order to determine the most suitable technology, and therefore the ideal frequency to use.

2.6.1 Bluetooth

Bluetooth is a communications technology originally developed as a wireless alternative to the RS-232 standard [27]. It makes use of the 2.4 GHz ISM band and has output power of 5-20 dBm with a range of 10-100 m. Bluetooth is used extensively by wireless mobile equipment and computer peripherals. Because of its extensive use in consumer electronics, Bluetooth may experience interference if used for electronic monitoring. The short range of Bluetooth may also limit the usability of a Bluetooth-based electronic monitoring system. Although Bluetooth is not especially high-powered, to get a useful range out of a Bluetooth device the power output of the transmitter will need to be at the maximum of 20 dBm. Bluetooth version 4 specifies the requirements for a low-power Bluetooth device [27] that will deliver similar performance to earlier Bluetooth revisions. This does not compensate for the other drawbacks experienced by Bluetooth. Another drawback of Bluetooth is the licensing fees required to use Bluetooth technology.

2.6.2 Wi-Fi

Wi-Fi is a full-duplex communication technology used mainly for wireless networking [28]. It makes use of the 2.4 GHz and 5.8 GHz ISM bands. "Wi-Fi Certified" devices are able to communicate with one another. Since it has a limited power output of 20 dBm, it has limited range when not making use of external, high-gain antennas. Typical range is about 30 m indoors and approximately 100 m outdoors. The 2.4 GHz

band will suffer from similar interference problems as Bluetooth. The 5.8 GHz band is not as congested as the 2.4 GHz band, but the higher frequency means poorer propagation characteristics. Another problem with Wi-Fi is its high power usage. It was not developed for low-power applications and therefore it is not ideally suited for use in electronic monitoring.

2.6.3 Wireless sensor technology

A Wireless Sensor Network (WSN) is made up of a number of distributed autonomous sensors to monitor a wide range of parameters [29]. WSNs are usually implemented in environments where the sensors are hard to access and therefore they need to operate efficiently for extended periods of time. To achieve this, the sensor nodes used in WSNs are low-power devices which operate on one of the lower ISM bands, usually 434 MHz. This is to ensure the best possible propagation is achieved [30]. Some of the more prevalent WSN standards are discussed in the following sections.

2.6.3.1 Zigbee

Zigbee is a specification for the communication protocol used by very small, low-power radio transmitters for use in Personal Area Networks (PANs) and WSNs [31]. It is extensively used in home automation. It operates on various frequencies, including 868 MHz, 915 MHz and 2.4 GHz, and is a very flexible option. The main drawback of using the Zigbee protocol is licensing, controlled by the *Zigbee Alliance*. Zigbee may only be used license-free for non-commercial applications.

2.6.3.2 WirelessHART

WirelessHART is the wireless implementation of the Highway Addressable Remote Transducer (HART) protocol, mainly used for digital industrial automation control [32]. The WirelessHART technology makes use of a mesh network for communica-

tion on the 2.4 GHz ISM band. By limiting the size of the tethering device connected to the ankle of the offender, the available resources are very limited, making it hard to implement WirelessHART.

2.6.3.3 Proprietary protocol

Zigbee and WirelessHART are two of the most widely implemented standards currently in use. Since both of these protocols are of limited use in the electronic monitoring system, the following question arises: Is it possible to develop and use a proprietary communications protocol by using the best that both Zigbee and WirelessHART has to offer?

The frequency to be used should be part of the ISM or other license-free frequency bands. The 2.4 GHz ISM band should be avoided if possible, since it is rather congested and leads to a very noisy environment that may hamper proper operation of an electronic monitoring system. 433 MHz is part of the ISM bands and is less congested than the 2.4 GHz band. The lower frequency also propagates better and is less susceptible to signal blocking due to the higher penetration achieved at this frequency. 868 MHz is not part of the ISM bands, but in South Africa it is a license-free band. Since it is not an ISM band and it is location specific to South Africa, there are not as many other commercial devices operating at this frequency and thus the channel quality is better than more congested alternatives. This may offset any problems experienced by the propagation of the higher frequency radio waves.

Both of these frequencies have advantages and disadvantages. 433 MHz propagates better through space; but the lower frequency implies a larger wavelength and accordingly the antenna needed for proper operation must also be physically larger. Efficiency is sacrificed when using a smaller antenna at this frequency. Even though 868 MHz does not propagate as well as 434 MHz, the antenna used with it may operate at a higher efficiency due to the smaller wavelength and subsequent smaller physical size.

2.6.4 Decision regarding wireless technology

When looking at the different wireless technologies and protocols, it can be seen that there is a large number to choose from. Most of the aforementioned technologies and protocols are not suited for use in the electronic monitoring system due to licensing costs, lack of performance or high power usage. It was decided to make use of a proprietary protocol, since they are license-free, low-powered and deliver excellent performance.

2.7 Simulation tools

2.7.1 Overview of existing EM tools

Since simulation is a large part of the design process, it is important to understand the operation of the tools used to simulate the antenna structure. This is especially important as there are numerous simulation methods and software packages available and the most suitable one needs to be chosen. There are two important questions that should be asked before a final decision is made regarding the simulation package to use:

- What must be simulated?
- In what environment must the simulation take place?

Some of the most common simulation packages will now be discussed before a final decision is made in this regard.

2.7.1.1 Method of moments

The Method of Moments (MoM), or Boundary Element Method (BEM) as it is sometimes known as, is a numerical technique for solving linear partial differential equations formulated as integral equations. It is widely used in engineering sciences and is

very popular for simulating electromagnetics [33]. From the name it can be deduced that this technique only calculates boundary values, instead of values throughout the problem space. MoM is therefore more efficient in terms of computational resources necessary to solve the problem if the surface-to-volume ratio of the problem space is relatively small. The MoM is used mainly for problems in linear homogeneous media. The electromagnetic sources are the quantities of interest and thus MoM is useful for radiation and scattering problems. The main drawback of this technique is that the computational time and storage increases by the square of the problem. Because MoM only calculates values on the outside border of the problem space, it may be less accurate than methods calculating values throughout the entire problem space [34].

2.7.1.2 Finite-difference time-domain

The Finite-Difference Time-Domain (FDTD) technique is a time-based technique and therefore a wide range of frequencies can be covered by a single simulation run [35]. It is also easy to understand and implement in software. The partial differential form of Maxwell's equations are modified into central-difference equations, discretised and implemented. The equations are first solved for the electric field, then for the magnetic field (since the H-field is the curl of the E-field). This cycle is then repeated until the complete problem space has been solved. This holds true for one-dimensional, two-dimensional and three-dimensional FDTDs. It becomes rather difficult to calculate the curl numerically when considering a multi-dimensional problem space. One solution to this problem is the creation of the lattice of Yee cells (Figure 2.21) throughout the problem space. By solving for the **E**-field and the **H**-field separately, simultaneous calculations can be avoided. Certain simulations could however need several time-steps to complete the process of solving the simulation.

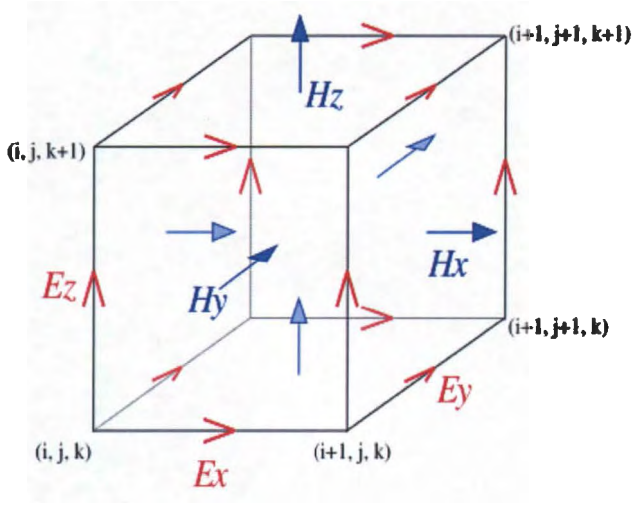

Figure 2.21: Cartesian Yee cell

2.7.1.3 Finite element method

The Finite Element Method (FEM) is a numerical technique in finding approximate solutions to Partial Differential Equationss (PDEs) as well as integral equations. The PDEs are approximated by a system of ordinary differential equations and solved numerically by making use of numerical techniques, like Euler's method, Newton approximations or Runge-Kutta. The FEM is a good choice for solving these ordinary partial differential equations in complex solution spaces [36].

The first step when making use of the FEM is the discretisation of the solution region into smaller sub-regions, called finite elements. The dimensions of the finite elements are dependent on the dimensions of the complete problem space. Some typical finite elements for the one-dimensional, two-dimensional and three-dimensional problem space are illustrated in Figure 2.22. The equations for each element is then derived and solved. The solution of one element serves as the input for the next element. It is for this reason that the entire problem space is divided into a mesh of finite elements and not just the boundary. The computational and storage requirements increase linearly as the problem space increases. The FEM is more accurate in doing calculations in a small problem space compared to MoM, but if the problem space increases in size, it might be impossible to make use of FEM.

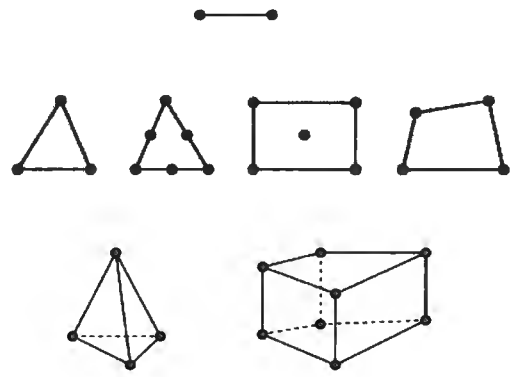

Figure 2.22: Typical 1-D, 2-D and 3-D finite elements [37]

2.7.1.4 Hybrid method

Due to the limitations of both MoM and FEM, a hybrid model consisting of both methods may be an ideal solution. This works especially well if multiple objects are placed a reasonable distance from one another and needs to be simulated [34]. Each object may be solved using the FEM, while a boundary surrounding each object will be solved using MoM. The solutions obtained from the FEM will act as input to the boundary calculations. The space between the objects can be assumed to be free-space and treated as a linear homogeneous material. The boundary values of each object will then interact with each other through this linear homogeneous material, thereby solving the problem.

2.7.2 Selected simulation package

From section 2.7.1 a general overview of the most popular methods for solving computational electromagnetic problems was obtained. There is a wide variety of simulation packages available that incorporates these methods to solve various electromagnetic problems. SuperNEC is a popular simulation package making use of MoM. A wire frame is drawn of the structure to be simulated, after which the boundary is solved.

It is primarily used to predict the HF near-fields, three-dimensional radiation patterns and antenna-to-antenna coupling. Complex microstrip structures or antennas that are electrically small can not be accurately simulated with SuperNEC. Another simulation package that is widely used is Ansys High Frequency Structure Simulator (HFSS) [38], making use of the FEM to solve EM problems. FEKO is a simulation package primarily making use of MoM, but also of a hybrid FEM/MoM model that ensures full coupling between a FEM region and a MoM boundary.

A decision was made to use the Ansoft HFSS simulation package. There are good reasons why it is ideally suited:

- **Structure Size:** Since the size of the antenna structure is limited by the constraint placed on the OID, it can be assumed that the antenna will be electrically small. MoM is therefore unsuitable for this problem;
- **Computer Resources:** The boundary placed around the antenna structure is critical when making use of FEM. The size of the antenna for the OID should however be small enough to limit the amount of computer resources necessary to find a solution to this problem.

2.7.3 Optimisation and parametrisation

Ansoft HFSS supports both optimisation and parametric sweeps. When designing a high-frequency structure, doing a parametric sweep of various design variables will create design curves which can be used to narrow down the design of the correct structure. One example of a parametric sweep is to sweep the length of a dipole antenna. Plotting the Voltage Standing Wave Ratio (VSWR) for S_{11}, as depicted in Figure 2.23, for the various sweep lengths will give a general idea of the lengths at which the dipole antenna resonates for a specific frequency.

When doing an optimisation in HFSS, the design boundaries are set for the problem, after which the optimisation value is set. The design boundaries may refer to the fre-

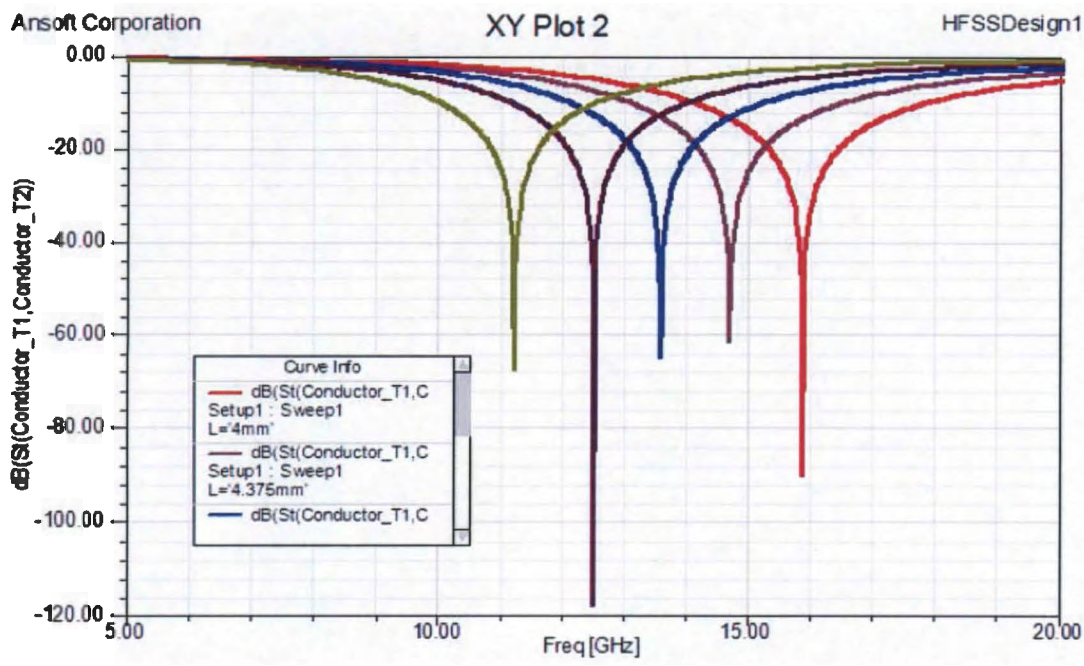

Figure 2.23: Parametric S_{11} plot

quency range, physical antenna structure size or optimised value. If the same example of the dipole antenna is used, the maximum and minimum lengths for the antenna are specified, as well as the step size for the optimisation of the size. A desired outcome is also specified for the optimisation. If multiple outcomes are expected, or desired, each outcome is specified together with a weight to determine the importance of each outcome.

2.8 Chapter review

In this chapter, concepts regarding EM waves were discussed. These included the properties of EM waves as well as environmental effects influencing wave propagation. Different channel models were investigated in order to decide on the best model to use when evaluating the antenna designed for use in the electronic monitoring system. Various types of antennas were discussed together with their characteristics.

A decision was made regarding which antenna type to use as well as possible operating frequencies. To summarise, the Transformer Coupled Loop (TCL) antenna was chosen for its small size while retaining relatively high efficiency. In terms of frequencies, 433 MHz and 868 MHz were chosen as possible operating frequencies due to their various licensing and propagation characteristics. Different simulation software packages were also discussed together with their operating methods. Due to the constraints placed upon this design, it was decided to use the Ansoft HFSS software to simulate the antenna design.

Chapter 3

Methodology

In this chapter the methodology used to design the antenna is discussed, as well as the procedure that will be followed to verify and validate its operation

---

3.1 Introduction

Figure 3.1 indicates the methodical approach followed in the design of the antenna. The constraints and requirements indicated in Figure 3.1 were discussed in Section 1.2. The resources refers to the tools used to accomplish the task of designing the antenna, and it includes antenna EM simulation tool. The output in Figure 3.1 is a functional antenna. The purpose of this chapter is to explain the process used to develop the antenna.

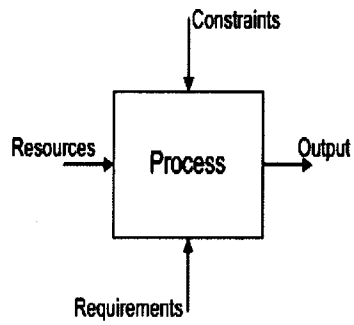

Figure 3.1: Design methodology

3.2 Design process

The process element in Figure 3.1 can be expanded into Figure 3.2. The subsections that follow explain each of the process blocks in Figure 3.2, with the number of each block corresponding to the appropriate subsection.

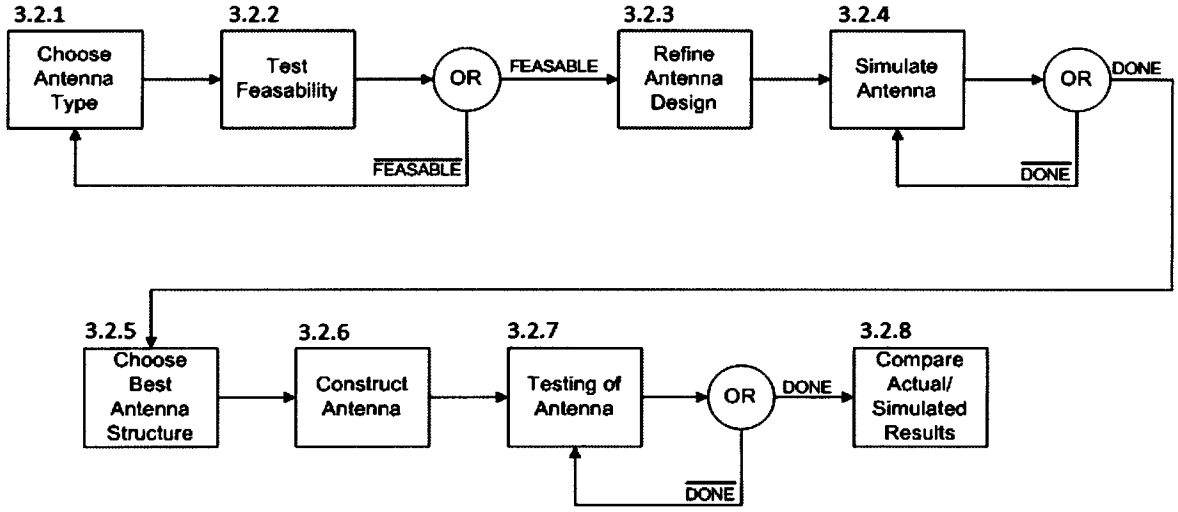

Figure 3.2: Antenna design process

3.2.1 Choose antenna type

Throughout Chapter 2, the importance of choosing the correct type of antenna was discussed. The first step in the design process is therefore the decision as to which type of antenna to use, and a TCL antenna was selected (see Section 2.5.4). The antenna that will be used will influence the rest of the design process. The requirements of the OID led to certain constraints being placed on the antenna. The constraints placed on the design will determine the dimensions and type of antenna structure to use. The antenna structure refers to the physical implementation of the TCL antenna.

3.2.2 Test feasibility of antenna design

It is possible for a broad variety of antenna structure variations to be used in the OID. Not all of these antenna structures will yield the required performance or conform to the constraints placed on the antenna. It is therefore necessary to test the feasibility of the antenna design. To build and test every antenna structure is expensive and time-consuming. A simpler method for doing this is by making use of antenna simulation software, where the antenna structure can be designed to comply with the size constraints of the OID. If the size of the antenna structure is correct, it can be simulated to test its performance. The antenna structure should be able to resonate at the chosen frequencies and it should not be overly directional, since this will limit its use in the OID. The resonance of the antenna is illustrated by means of a VSWR plot of S_{11} of the antenna structure (illustrated in Figure 3.3)

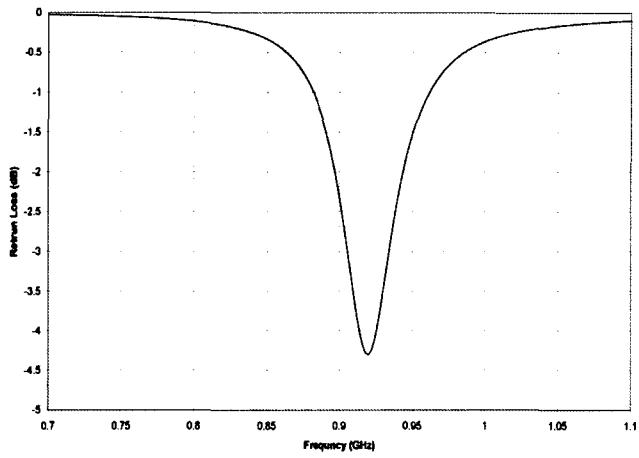

Figure 3.3: S_{11} plot

3.2.3 Refine antenna design

The next step in the design process is the refinement of the antenna design. In the previous step, the feasibility of various antenna structures was investigated. Some antennas were disqualified from use in the OID, while others proved to be feasible. The broad range of antennas has thus been narrowed down to a select few. The antennas remaining should be carefully analysed, and the designs refined all the while staying within the constraints.

3.2.4 Simulate antenna

The refined antenna design will be thoroughly tested. This is done by doing a detailed simulation of every antenna design. It is important to simulate the different antennas as accurately as possible. The simulated environment will also be important, as a more accurate simulated environment will lead to more accurate simulation results, comparable to the results obtained when testing the physical antenna. Accurate results will lead to the most desirable antenna being implemented.

3.2.5 Select optimal antenna

After all simulations have been completed, a decision needs to be made regarding the optimal antenna to use. To establish which antenna structure is the best, the performance of the antenna structure must be quantifiable. To this end two important antenna parameters were chosen:

- **Resonance:** The simulations should provide enough data as to which antenna structure has the best resonance. The maximum amount of electrical energy should be converted to EM energy;
- **Gain:** The simulation should also provide data as to the gain of each antenna structure. For example, an antenna structure with a gain of 0 dB is more useful than an antenna structure with a gain of -10 dB.

If the desired performance of the antenna is reached, and the design of the antenna is within the desired design constraints, the antenna design can be considered successful.

3.2.6 Construct antenna

The constraints mentioned in Chapter 1 should be taken into consideration:

- The size of the Printed Circuit Board (PCB) is the same as used in the simulation.
- The substrate material used for the PCB is FR4 laminate, and the thickness of the copper traces is 35 μm;
- The antenna is cut from metal sheets with high conductivity.

It is not necessary to design and build a transmitter for the test platform. It will be sufficient to buy a transmitter for this use, as long as the transmitter used has similar specifications for both 434 MHz and 868 MHz.

3.2.7 Testing of antenna

It is important to test the antenna using different test scenarios. These tests are limited to:

- Antenna characterisation test;
- Human proximity test.

The antenna characterisation tests will be used to find the horizontal and vertical radiation patterns. Furthermore, it is important to test the antenna in a real-world environment, if possible. This can be done by placing the antenna and transmitter in an enclosure, similar to the one used by the OID, placing it on a person's leg and measuring antenna performance over a period of time while the person moves around a chosen environment. One of the ways in which the antenna performance can be measured is by using a human analogue to test the antenna characteristics. A good human analogue to use is a saline solution vaculitre bag, the electrical characteristics of the saline solution is a close approximation off the electrical characteristics of the human body. It should be remembered that to achieve the best results, the tools used to test the antenna should not interfere with the tests.

3.2.8 Compare results

The final step in the design process is the comparison of the measured results with simulated results. This is especially important to validate the performance of the chosen antenna design within the electronic monitoring system. The measured radiation pattern and three-Dimensional gain pattern of the antenna should be similar to that of the simulated antenna. The bandwidth and resonant frequency of the actual antenna should also match the simulated antenna. All of this forms part of the validation stage of the design.

3.3 Chapter review

This chapter discussed the design process to be followed in detail, with explanations of every step givens. The importance of design decision were also discussed as well as the influence these decisions has on the antenna design. The testing and validation procedure were also briefly discussed.

Chapter 4

Design and simulation

The design and simulation of the antenna structure is discussed together with the simulation results.

4.1 Introduction

The theoretical design of the antenna is done in this chapter. This design is done with all of the requirements and constraints, as discussed in Chapter 1, as inputs to the design. After the design is done, variations on the theoretical design is simulated to see which variation will deliver the best results.

4.2 Theoretical antenna design

In Chapter 2 the decision was made to use the TCL antenna and make use of Ansoft HFSS software to simulate the antenna. The theoretical design discussed in this section was done before simulating any variation on the antenna structure. Preliminary sim-

ulations were done on various antenna structures after the theoretical design in order to eliminate unsuitable antenna structures. Figure 4.1 is a schematic representation of the TCL antenna. L_{AP} is the length of the primary loop and L_{BP} is the width of the primary loop of the antenna. Similarly L_{AS} is the length of the secondary loop and L_{BS} the width of the secondary loop of the antenna. The length and width of both the primary and secondary loops should be chosen as practical values for the system it is used for.

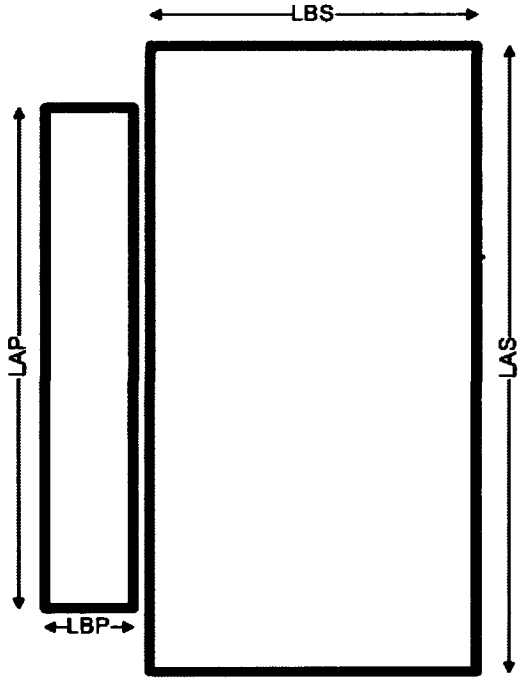

Figure 4.1: Transformer coupled loop antenna

The steps in designing a TCL antenna are as follows:

- Given the dimensions of the antenna, the radiation resistance (equation 4.1) and loss resistance (equation 4.2) of both the primary and the secondary loop need to be calculated;

$$R_{rad} = (3.84 \times 10^{-30})(L_{Ax}L_{Bx})^2 f^{4*} \tag{4.1}$$

*x refers to either the primary or the secondary loop

$$R_{loss} = \frac{L_{Ax} + L_{Bx}}{w}(2.61 \times 10^{-7})\sqrt{f} \tag{4.2}$$

- The efficiency (equation 4.3), gain (equation 4.4) and loop inductance (equation 4.5) of the antenna structure can be calculated;

$$\eta = \frac{R_{rad}}{R_{rad} + R_{loss}} \tag{4.3}$$

$$Gain = 10\log_{10}(\eta) \tag{4.4}$$

$$L_{Loop} = \frac{\mu}{2\pi} l \ln(\frac{8A}{lw}) \tag{4.5}$$

- Calculating the mutual inductance (equation 4.6) of the loops is next, as this is important for the impedance transformation;

$$M = \frac{\Phi}{I_s} = \frac{\mu_0 L_{AP}}{2\pi} \ln(1 + \frac{L_{BP}}{L_{offset}}) \tag{4.6}$$

- Finally, the input impedance (equation 4.7) is calculated for the given antenna structure. To simplify the problem, only the real part (equation 4.8) may be used to calculate the input impedance.

$$Z_{IN} = (R_p + \omega^2 M^2 \frac{R_s}{R_s^2 + X_s^2}) + j(X_p + \omega^2 M^2 \frac{X_s}{R_s^2 + X_s^2}) \tag{4.7}$$

$$Z_{IN} = (R_p + \omega^2 M^2 \frac{1}{R_s}) \tag{4.8}$$

Table 4.1 gives the theoretical results when the aforementioned equations were used to solve for the desired frequencies and a realistic size.

Table 4.1: Antenna calculations

f	868 MHz	434 MHz
λ	0.345 m	0.691 m
ω	5453804847 rad/s	2726902423 rad/s
L_{AS}	40 mm	40 mm
L_{BS}	28 mm	28 mm
L_{AP}	28 mm	18 mm
L_{BP}	18 mm	1.6 mm
W_S	2 mm	2 mm
W_P	1.25 mm	1.25 mm
σ	5.8×10^7 Ω /m	5.8×10^7 Ω /m
μ	1256.637 nH/m	1256.637 nH/m
$Area_S$	0.00112 m^2	0.00112 m^2
$Perimeter_S$	0.136 m	0.136 m
$Area_P$	0.0000288 m^2	0.0000288 m^2
$Perimeter_P$	0.0392 m	0.0392 m
R_{LOSS_S}	0.261 Ω	0.145 Ω
R_{RAD_S}	2.734 Ω	0.349 Ω
R_{LOSS_P}	0.121 Ω	0.0853 Ω
R_{RAD_P}	0.00181 Ω	0.000113 Ω
Efficiency	0.72	0.2696
Gain	-1.425 dB	-5.693 dB
M	6.522 nH	6.522 nH
Z_{IN}	333.404 Ω	244.539 Ω

4.3 Parameters simulated

There are various parameters that are important to the performance of the antenna that must be kept in mind. When comparing different antenna structures or doing an optimization on a single antenna design, the comparison of these parameters will allow for a decision to be made regarding which antenna structure to physically implement. These parameters are:

- **Resonance:** The chosen antenna structure should resonate at the correct frequency, or should be able to be made to resonate at the correct frequency by making use of tuning components;
- **Impedance:** The closer the impedance of the antenna structure is to 50Ω, the easier the external antenna matching will be;

- **Gain/Directivity:** Ideally the antenna should be as close as possible to an omni-directional antenna, thus not have a lot of gain/directivity in one direction;
- **Polarisation/Diversity:** The antenna structure chosen should exhibit some spatial or polarisation diversity;
- **Sensitivity to human proximity:** Since the OID will be fitted to a person, the sensitivity of the antenna structure to the proximity of the human body should be incorporated into the antenna design.

4.4 Simulated antenna models

4.4.1 Standard magnetic loop antenna

When designing a variation of a loop antenna, it is important to compare it to an optimal loop antenna design. The new design should be compared to a known quantity, like the theoretical standard loop antenna, which has known characteristics. The performance of the proposed design can then be compared to the known performance of the standard loop antenna.

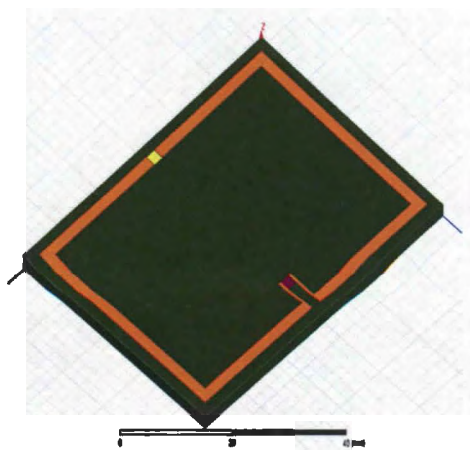

Figure 4.2: Standard magnetic loop antenna

The loop antenna depicted in Figure 4.2 was simulated on the same size and type of

PCB as used with all of the antenna designs. This will ensure that a direct comparison can be made. A differential port (in purple) is used together with a tuning component (in yellow) that may be either a capacitor or an inductor, depending on the structure and operating frequency.

Figures 4.3 and 4.4 shows the radiation pattern for the loop antenna for 434 MHz and 868 MHz when plotting the gain of the antenna in dB. The figures look similar with the only difference being the maximum gain obtained. At 434 MHz, the maximum gain is approximately $-7dB$, while for 868 MHz the maximum gain is approximately $-1dB$.

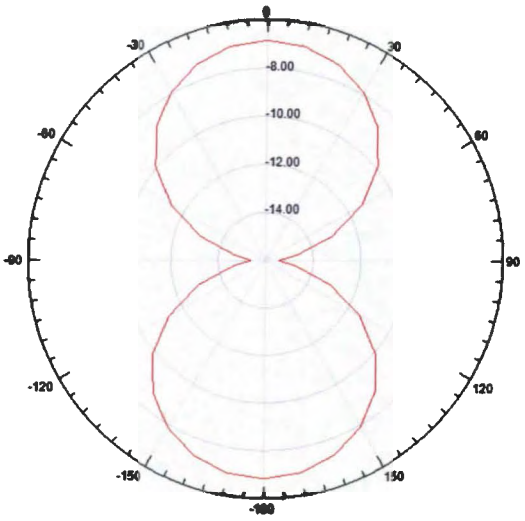

Figure 4.3: 2-D radiation plot - 434 MHz

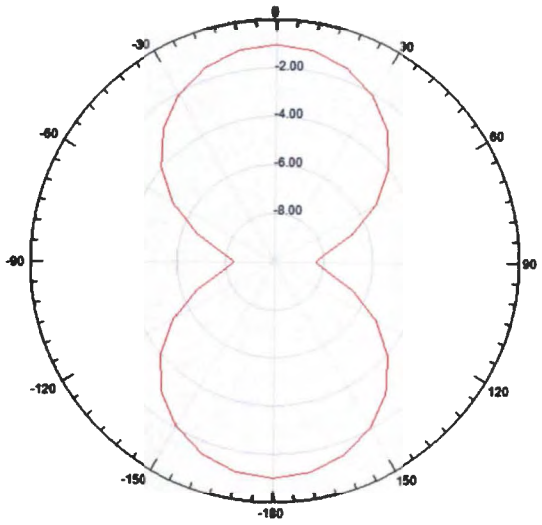

Figure 4.4: 2-D radiation plot - 868 MHz

The three-dimensional gain plots shown in Figures 4.5 and 4.6 again shows little difference between the two frequencies, except for the maximum gain achieved.

Figure 4.7 shows the S_{11} data for both frequencies. This is where the biggest difference between the two frequencies can be observed. If a minimum is achieved at the operating frequency, the structure is said to be resonating and the maximum amount of power is radiated by the antenna. For 434 MHz, the antenna structure could not be made to resonate,regardless of the tuning component used. It can be seen that the minimum value of $-5.6dB$ is achieved at a frequency of around 640 MHz with a bandwidth of 115 MHz. The bandwidth is f_{max} - f_{min} at the +3 dB point, where the +3 dB point is the upper- and lower frequency 3 dB higher than the resonating frequency. The most

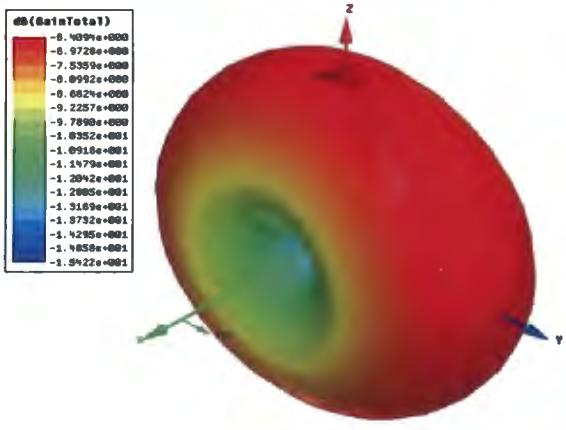

Figure 4.5: 3-D gain plot - 434 MHz

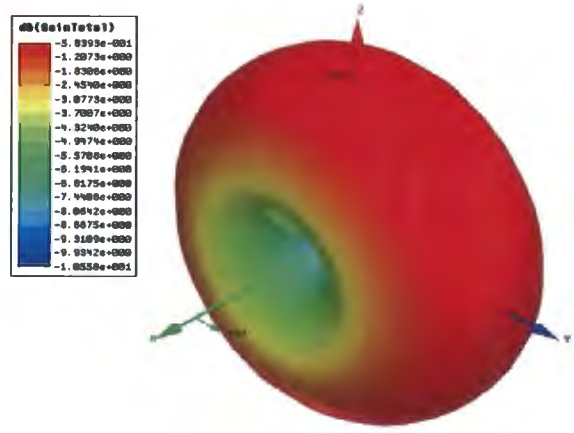

Figure 4.6: 3-D gain plot - 868 MHz

likely reason for the antenna structure not resonating at 434 MHz may be due to the small size. The circumference of this antenna is 196 mm, equal to about a quarter wavelength for 434 MHz. Ideally the circumference should be equal to one wavelength for a standard loop antenna. For 868 MHz the circumference is about 0.56λ. It was therefore much easier to get the structure to resonate, with an inductor value of 127 nH being used. The S_{11} data in Figure 4.7 shows that the structure resonates at 868 MHz with a bandwidth of 30 MHz. At 434 MHz the value of S_{11} is$-0.21dB$, while at 868 MHz the value is $-13.3dB$, therefore the structure resonates much better.

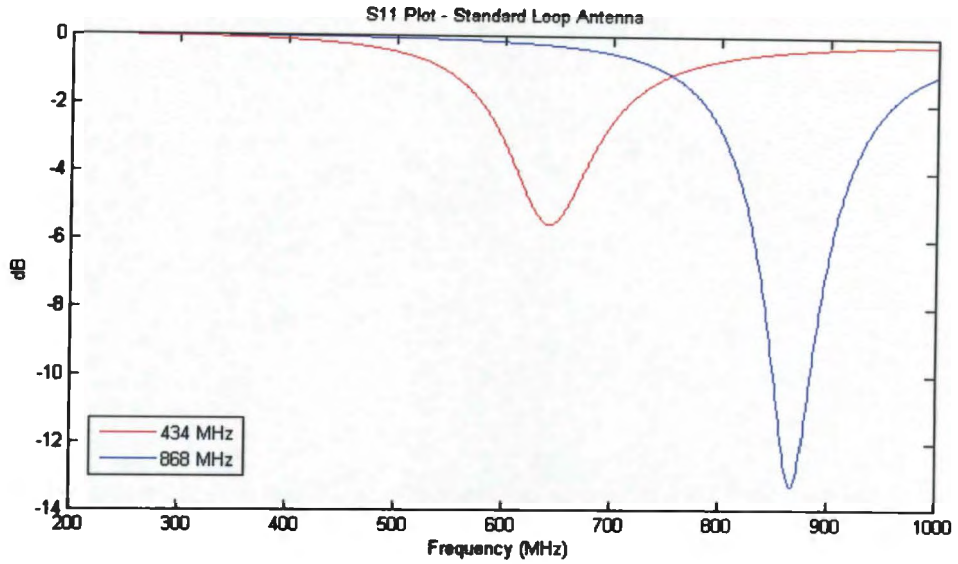

Figure 4.7: Comparison of S_{11} for 434 MHz and 868 MHz

4.4.2 Antenna with notch - Centre fed

Figure 4.8 shows an antenna structure, forming a "notch" over the primary loop, which is in the centre of the PCB. This will possibly make it easier to feed the two antennas if their feed points are close to one another. The notch adds mechanical support for the secondary loop, which consists of a tin structure set at a certain angle from the PCB substrate. This angle will allow for some spatial diversity between the two antennas.

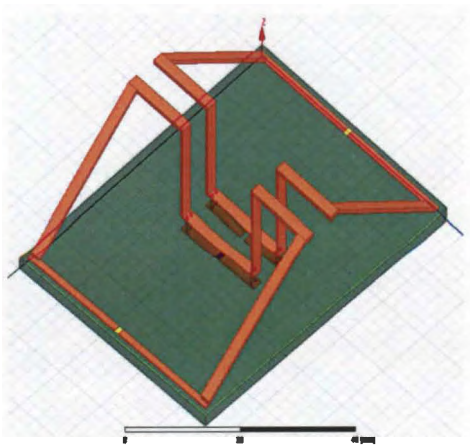

Figure 4.8: Antenna with notch - Centre fed

Figures 4.9 and 4.10 are the two-dimensional radiation patterns for this antenna when plotting the gain of the antenna structure, in dB. Although their shapes are similar, at 434 MHz it seems as if the antenna is more directional. The gain achieved for 868 MHz (-5.2 dBi) is better than for 434 MHz (-6.5 dBi), though not by much.

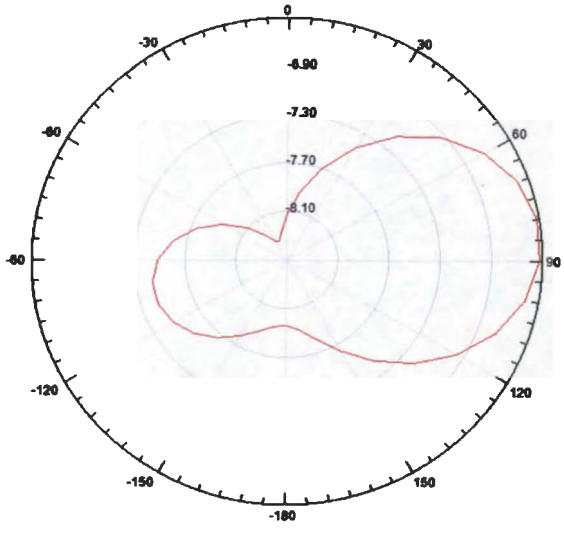

Figure 4.9: 2-D radiation plot - Antenna with notch - Centre fed - 434 MHz

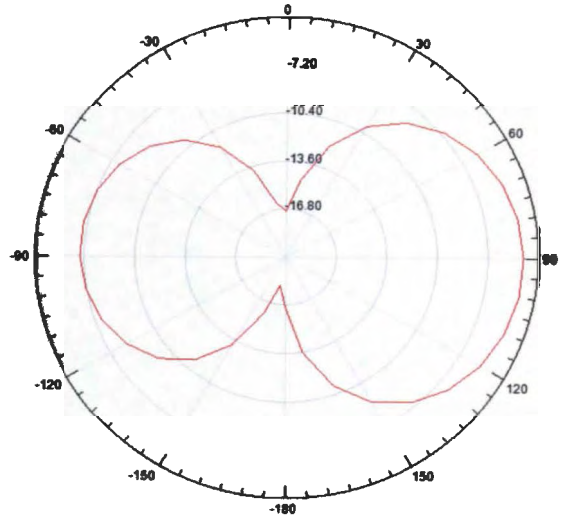

Figure 4.10: 2-D radiation plot - Antenna with notch - Centre fed - 868 MHz

The three-dimensional gain plots shown in figures 4.11 and 4.12 show a great difference between the two frequencies. Both have toroidal shapes, although the axis of the toroid is not the same for the two frequencies. For 434 MHz, a single antenna is electrically small. It is assumed that by placing another antenna of the same size in the near-field region of the resonating antenna, has allowed the second antenna to resonate as well. The energy radiated by both the antennas is combined to form the gain plot in Figure 4.11.

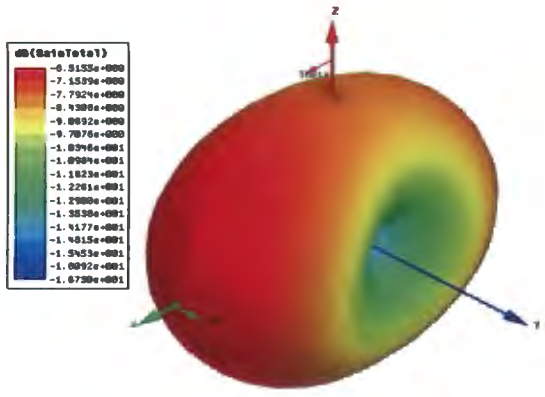

Figure 4.11: 3-D gain plot - Antenna with notch - Centre fed - 434 MHz

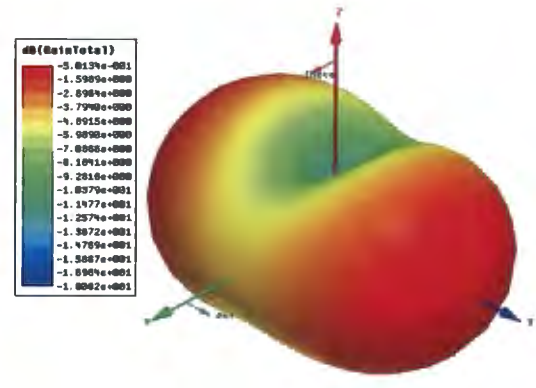

Figure 4.12: 3-D gain plot - Antenna with notch - Centre fed - 868 MHz

By studying Figure 4.13 for 434 MHz, it can be seen that there are two resonant frequencies with similar bandwidth and values for S_{11}. This gives credence to the assumption that there exists coupling between both structures and therefore they are both resonating, albeit at slightly different frequencies. For 868 MHz the size of a single antenna structure is closer to λ, and therefore there is less coupling between the two structures. This can also explain why its gain plot differs from the gain plot at 434 MHz. There are also two resonant frequencies, but the second frequency (780 MHz) is not as defined as at the desired frequency (868 MHz).

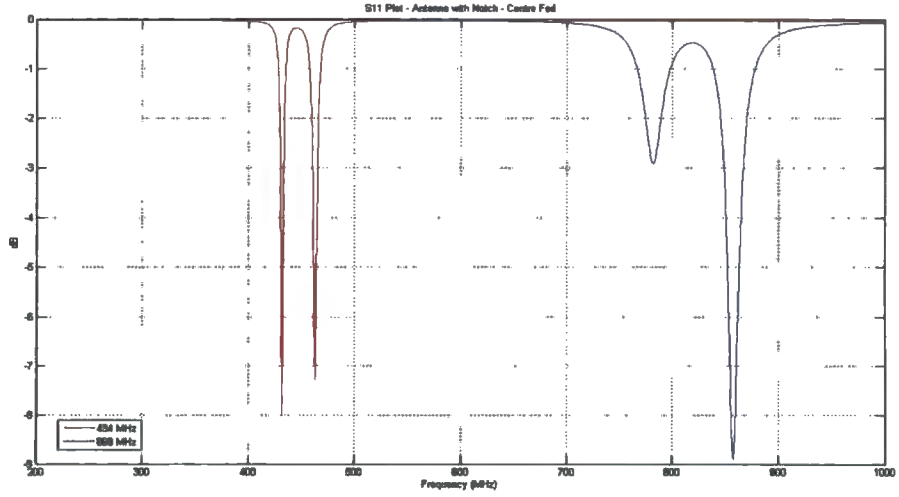

Figure 4.13: Comparison of S11 for 434 MHz and 868 MHz for Antenna with Notch - Centre fed

4.4.3 Antenna with notch - Outside fed

Figure 4.14 shows a structure similar to the previously discussed antenna, except for one difference. The primary loop, where the feed point is located, has been moved to the outside of the antenna structure, with the hope of reducing coupling between the two antenna structures.

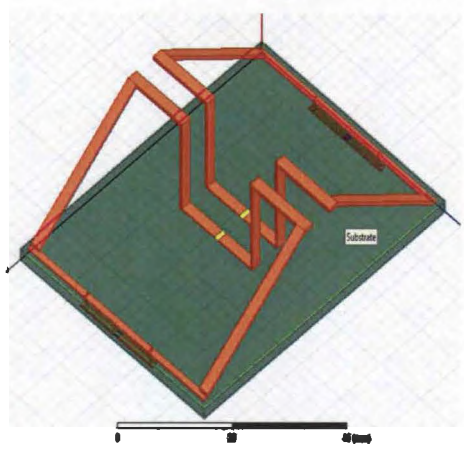

Figure 4.14: Antenna with notch - Outside fed

Again the two-dimensional gain pattern (in dB) for the chosen frequencies look similar (Figures 4.15 and 4.16). It should however be noted that the gain shown in the figures vary vastly, with the gain at 868 MHz at about 0.8 dB compared to about -9 dB at 434 MHz. This has to do with the size of the structure that is more ideally suited for use with 868 MHz, rather than 434 MHz.

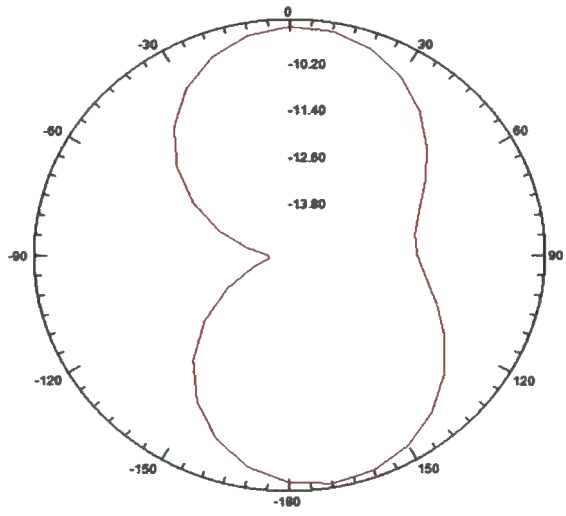

Figure 4.15: 2-D radiation plot - Antenna with notch - Outside fed - 434 MHz

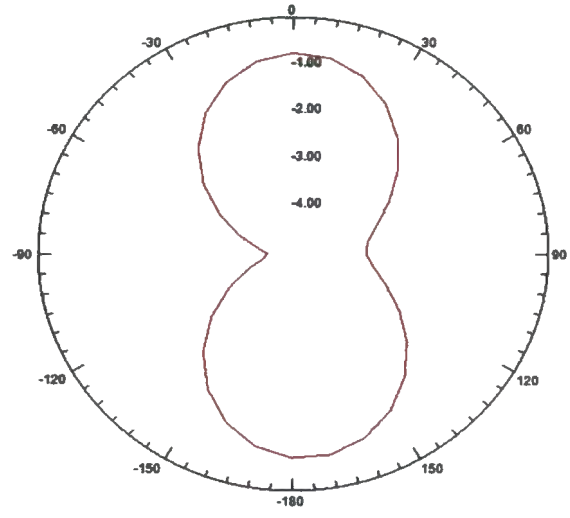

Figure 4.16: 2-D radiation plot - Antenna with notch - Outside fed - 868 MHz

Figures 4.17 and 4.18 shows similar toroidal shapes for the radiating structures. At 434 MHz the axis of the toroid is again different from the 868 MHz. The gain on the XY-plane is also less than for 868 MHz, making the antenna more directional at 434 MHz. In the direction of maximum gain, which is the Z-axis for both frequencies, there exists a 10 dB difference in gain between the two frequencies.

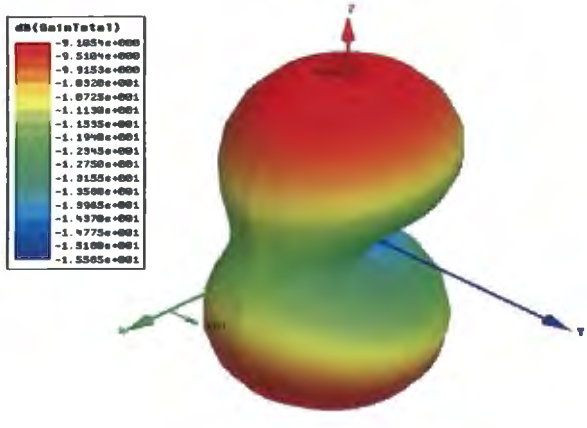

Figure 4.17: 3-D gain plot - Antenna with notch - Outside fed - 434 MHz

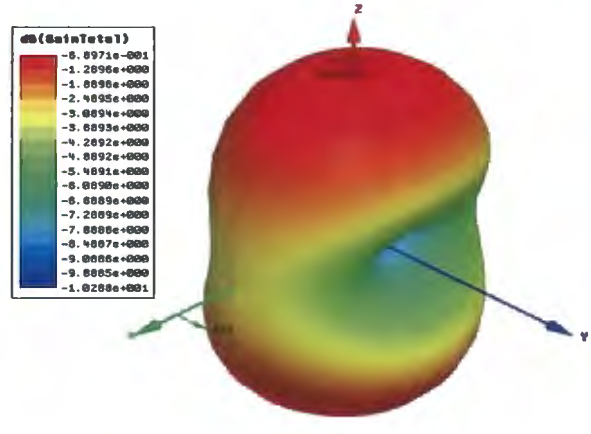

Figure 4.18: 3-D gain plot - Antenna with notch - Outside fed - 868 MHz

From Figure 4.19 it appears if the structures resonate better at 434 MHz (-17 dB) compared to 868 MHz (-7 dB). This should be taken into consideration if this antenna is decided upon.

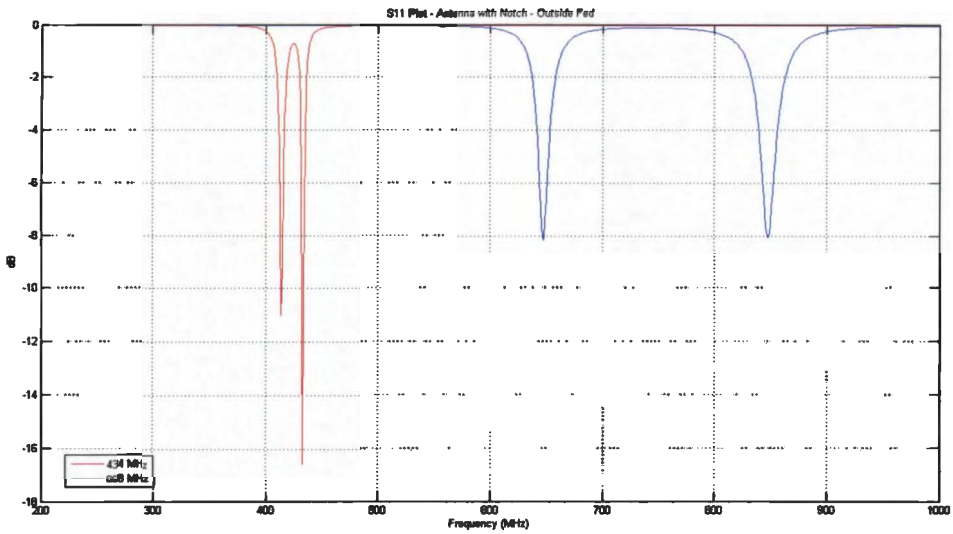

Figure 4.19: Comparison of S_{11} for 434 MHz and 868 MHz for Antenna with Notch - Outside Fed

4.4.4 Remarks regarding the antenna with notch

From the previous two antennas discussed, some interesting results were obtained.

- For both of the antenna structures improved performance is seen at 868 MHz compared to 434 MHz when comparing the radiation patterns and gain plots;
- If the primary loops are close to one another, when fed in the centre, the structure resonates equally well for both frequencies. If the primary loops are on the outside of the antennas, they resonate better at 434 MHz.

This is an important consideration when deciding upon an antenna structure to use.

4.4.5 Full loop antenna

The following three antennas are essentially the same, with only the size of the primary loop differing. This will illustrate the effect of the size of the primary loop on the performance of the antenna.

The first of these antennas, shown in Figure 4.20, has a primary loop width only slightly less than that of the secondary loop and the PCB. The general shape of this antenna is close to that of the theoretical TCL antenna shown in Figure 4.1, with the secondary loop placed at an angle to the PCB to ensure spatial diversity between the two antennas. Due to the design of the secondary loop (it has no supporting notch structure), the primary loop will always be on the outside of the PCB for this particular antenna design. This is why it is important to determine what the effect of the size of the primary loop is on antenna performance.

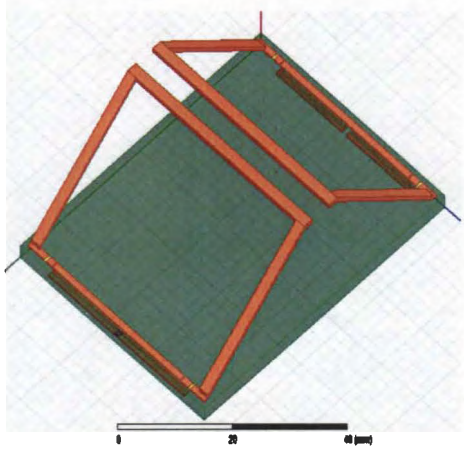

Figure 4.20: Antenna without notch - Full primary loop

From Figures 4.21 and 4.22 it can be seen that their radiation patterns are similar to one another, when looking at the gain of the antenna, in dB. Even the maximum gain achieved at both frequencies has a difference of about 3 dB.

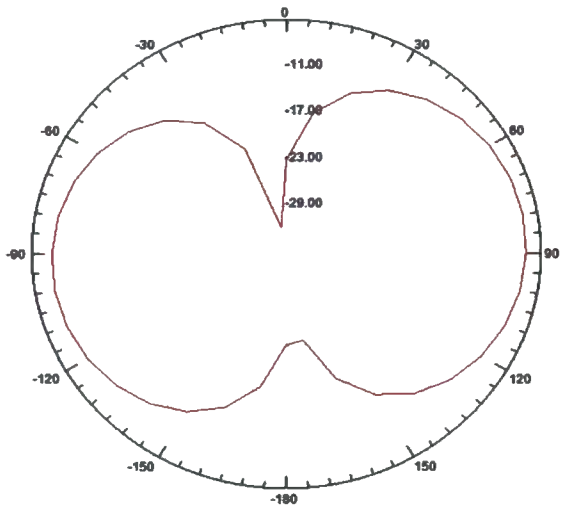

Figure 4.21: 2-D radiation plot - Antenna with full primary - 434 MHz

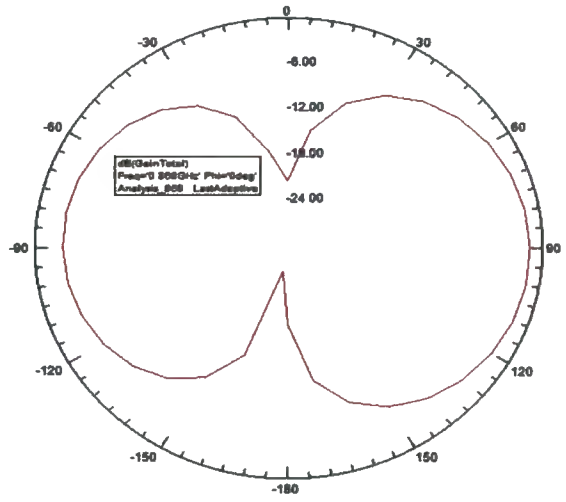

Figure 4.22: 2-D radiation plot - Antenna with full primary - 868 MHz

The three-dimensional gain plots (Figures 4.23 and 4.23) are almost exactly the same.

This time the difference in gain is equal to 6 dB, which is significant.

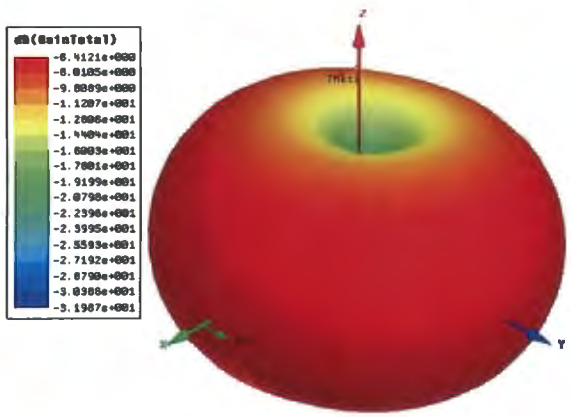

Figure 4.23: 3-D gain plot - Antenna with full primary - 434 MHz

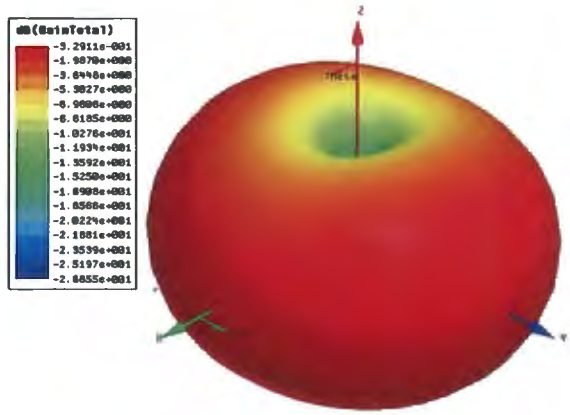

Figure 4.24: 3-D gain plot - Antenna with full primary - 868 MHz

Although the bandwidth at 868 MHz is not quite as good as at 434 MHz (Figure 4.25), it does resonate better.

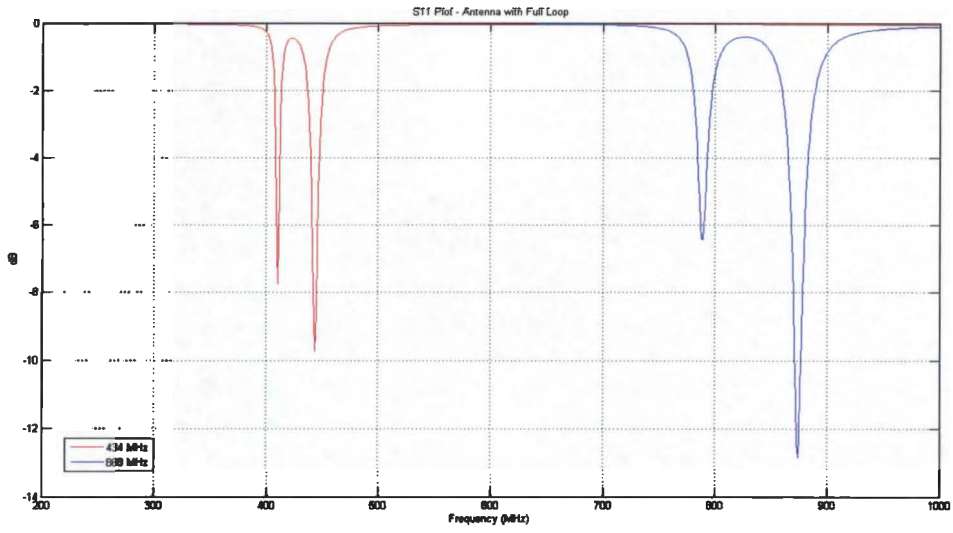

Figure 4.25: Comparison of S_{11} for 434 MHz and 868 MHz for Antenna with full primary loop

4.4.6 Half loop antenna

For the antenna shown in Figure 4.26, the width of the primary loop has been halved, compared to the previous antenna structure.

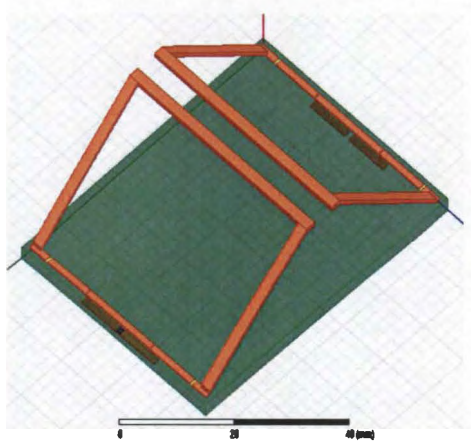

Figure 4.26: Antenna without notch - Half primary loop

The gain is again shown in dB for the radiation patterns. When looking at figures 4.27 and 4.28 the radiation patterns look similar to one another, and identical to those shown in Figure 4.21 and 4.22, where the primary loop had double the width. The gain values are also similar to those of the antenna discussed in Section 4.4.5.

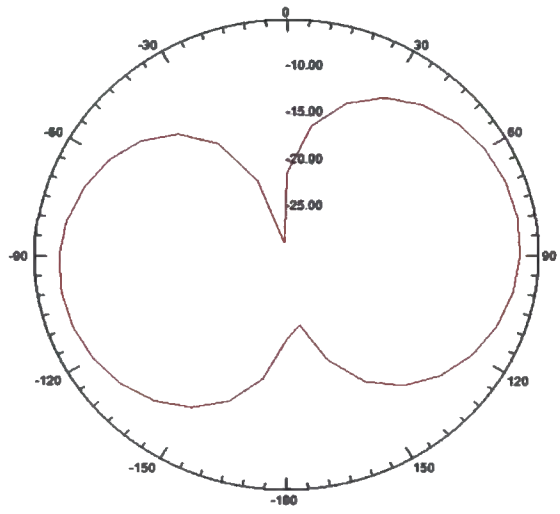

Figure 4.27: 2-D radiation plot - Antenna with half primary - 434 MHz

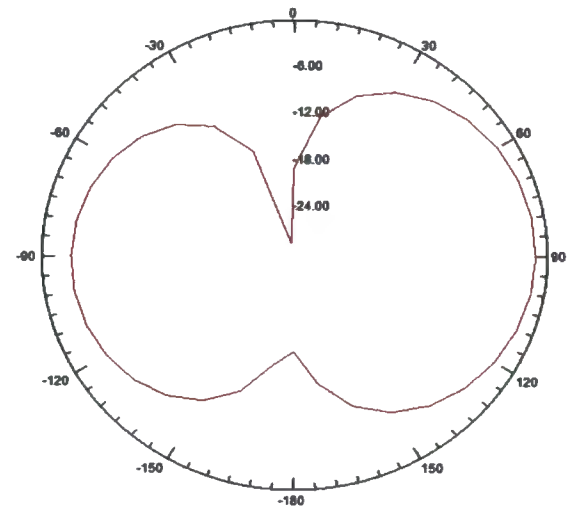

Figure 4.28: 2-D radiation plot - Antenna with half primary - 868 MHz

Looking at the three-dimensional gain plots (Figures 4.29 and 4.29) it can also be seen that they look similar with gain values similar to those previously obtained.

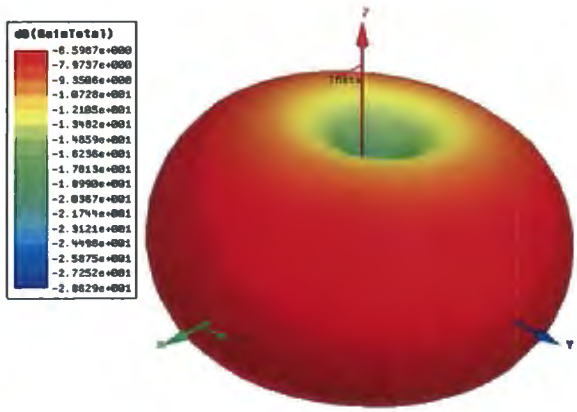

Figure 4.29: 3-D gain plot - Antenna with half primary - 434 MHz

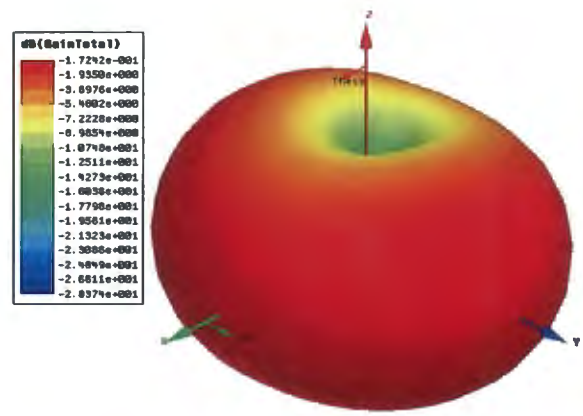

Figure 4.30: 3-D gain plot - Antenna with half primary - 868 MHz

The biggest difference is that this antenna structure resonates extremely well at 434 MHz, compared to 868 MHz (Figure 4.31).

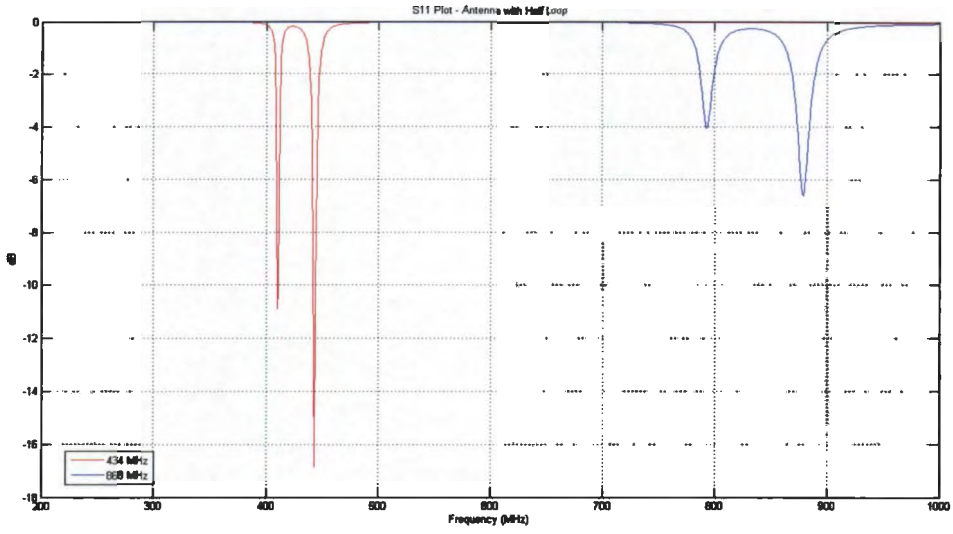

Figure 4.31: Comparison of S_{11} for 434 MHz and 868 MHz for Antenna with half primary loop

4.4.7 Quarter loop antenna

With this variation of the antenna, the width of the primary loop has been halved again (Figure 4.32), compared to the previous design. The width of the primary loop is thus a quarter of the width of the original loop.

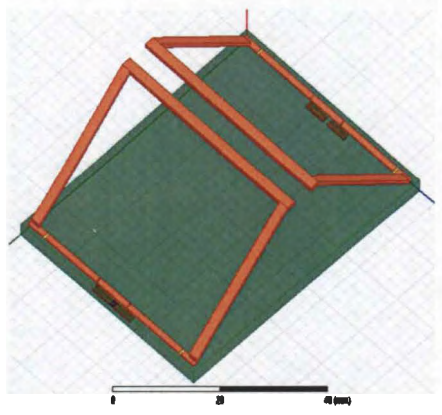

Figure 4.32: Antenna without notch - Quarter primary loop

From the radiation patterns shown in Figures 4.33 and 4.34 of the gain (in dB), the shape and gain for both frequencies are again similar. The only difference being that it seems as if the axis of pattern is tilted at 868 MHz.

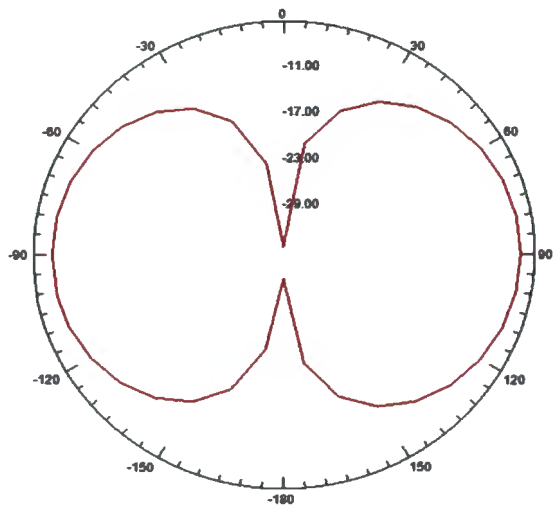

Figure 4.33: 2-D radiation plot - Antenna with quarter primary - 434 MHz

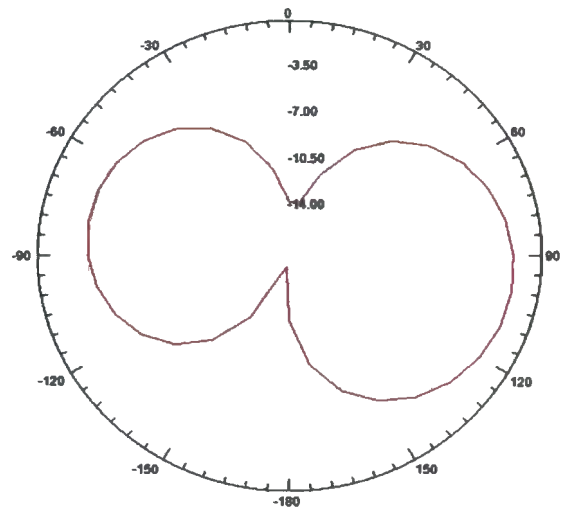

Figure 4.34: 2-D radiation plot - Antenna with quarter primary - 868 MHz

From Figures 4.35 and 4.36 it can be seen that at 868 MHz the antenna is slightly more directional, but not enough to make a substantial difference to antenna performance between the two frequencies.

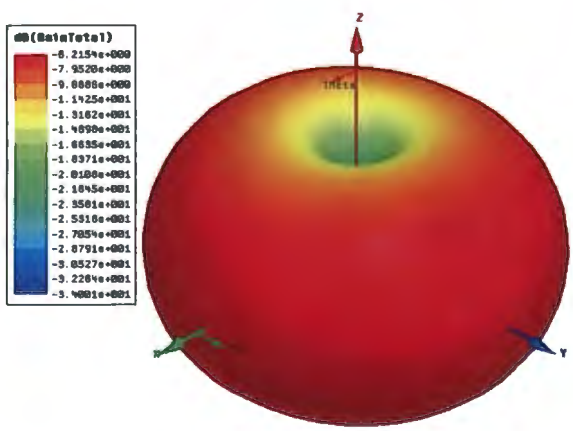

Figure 4.35: 3-D gain plot - Antenna with quarter primary - 434 MHz

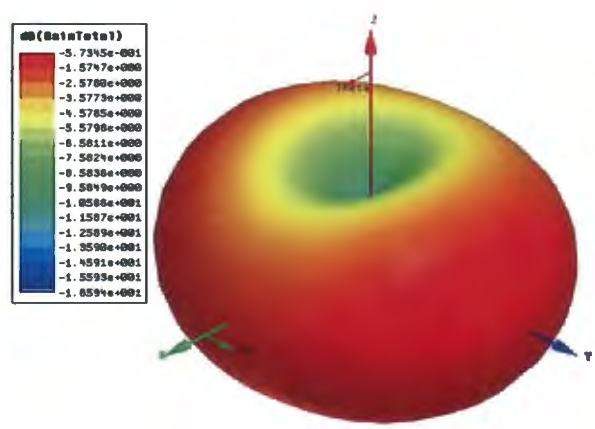

Figure 4.36: 3-D gain plot - Antenna with quarter primary - 868 MHz

Again it can be seen that with a smaller primary loop, the antenna structure resonates

better at 434 MHz (Figure 4.37). The bandwidth at 434 MHz is also much smaller and therefore delivers better selectivity.

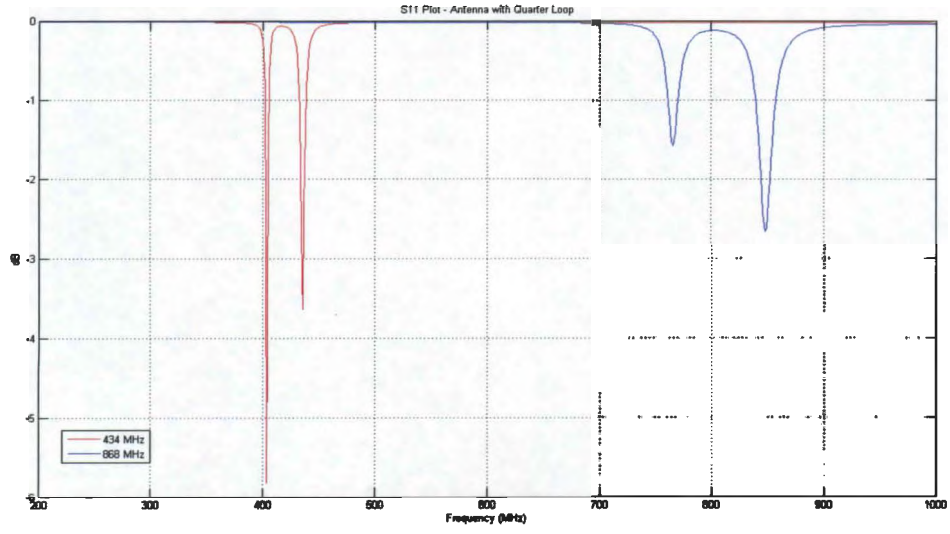

Figure 4.37: Comparison of S_{11} for 434 MHz and 868 MHz for Antenna with quarter primary loop

4.4.8 Remarks regarding the loop antenna

The antenna structure without the notch has delivered interesting results that should be carefully considered before a final decision is made regarding which antenna to use.

- The radiation patterns and three-dimensional gain plots look similar for all variations of this antenna;
- For the half- and quarter length primary loop, the antenna structure resonates better and has better bandwidth at 434 MHz;
- With a full length primary loop, the antenna structure resonates slightly better at 868 MHz than at 434 MHz. Even though the resonance at 434 MHz is not better than 868 MHz with a full loop, it is still the same as, or better than, resonance with a smaller primary loop.

4.5 Preferred antenna model

As mentioned in Section 4.3, there are various parameters and other criteria that should be considered before making a decision regarding which antenna to use. One of the most important parameters is directivity. Since this antenna will be used in a security application, it should not be highly directional. When looking at the three-dimensional gain plots of the different antenna designs, it appears that both of the antenna structures with the notch are more directional than the antennas without the notch. When looking at the VSWR on S_{11}, antennas without the notch resonates better than the antennas with the notch. Because of these reasons both of the notch antennas have been disqualified as possible solutions.

When looking at the results of the remaining antennas, it appears as if their performance is generally the same, no matter the length of the primary loop. When looking at the resonance of the various structures, the antenna structure with the maximum primary loop length resonates the best for both 434 MHz and 868 MHz, and is therefore the antenna of choice.

4.5.1 Optimisation of antenna model

As was mentioned earlier in this chapter, Ansoft HFSS has the ability to optimise a design. To ensure the best possible performance, the preferred antenna structure should be optimised. The S_{11} for both 434 MHz and 868 MHz should be a minimum with equal weights.

The optimised antenna has the following dimensions and is shown in Figure 4.38:

- PCB size: $58mm \times 46mm$;
- Primary Loop size: $21mm \times 1.6mm$;
- Secondary Loop size: $44mm \times 26mm$;

- Secondary Loop Height from PCB: 11 mm;
- Secondary Loop Angle of Tilt: 40.5° from horizontal.

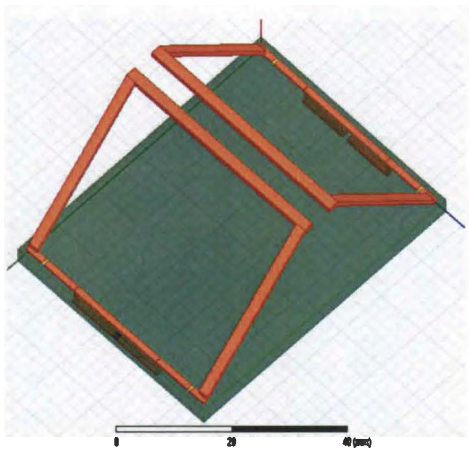

Figure 4.38: Optimised antenna for 434 MHz and 868 MHz

The 2-dimensional radiation pattern of the gain (dB) for the optimised antenna is shown in Figures 4.39 and 4.40. In the direction of maximum gain, both antennas has similar gain.

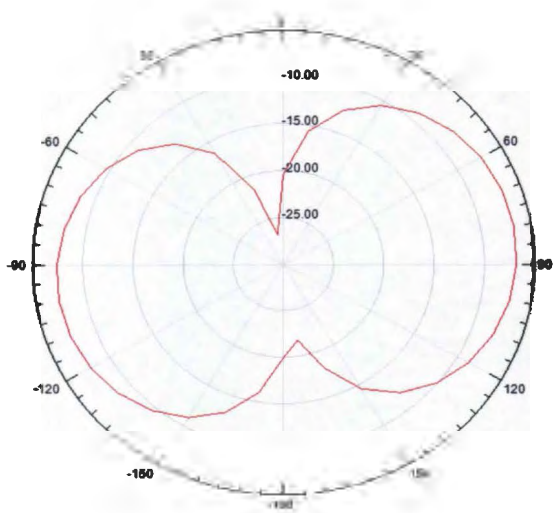

Figure 4.39: 3-D gain plot - Optimised antenna - 434 MHz

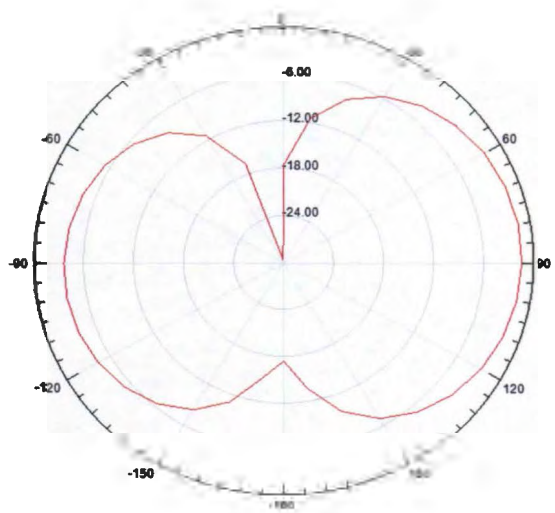

Figure 4.40: 3-D gain plot - Optimised antenna - 868 MHz

The three-dimensional gain plot illustrated for 434 MHz and 868 MHz in Figures 4.41 and 4.42 again shows that for both frequencies the gain is similar to one another.

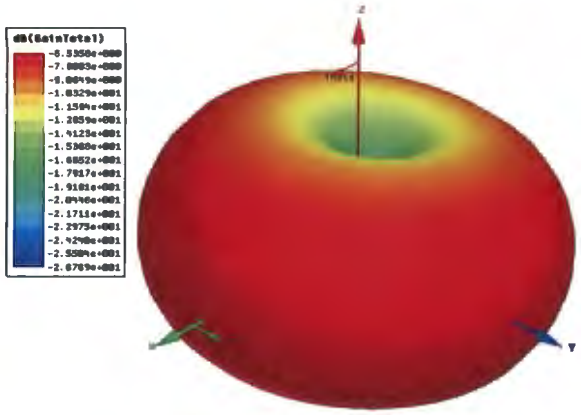

Figure 4.41: 3-D gain plot - Optimised antenna - 434 MHz

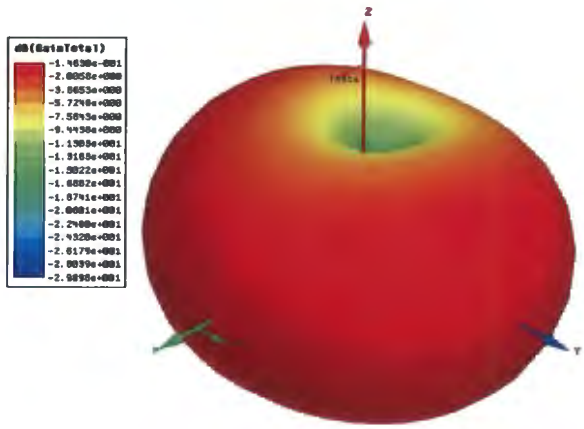

Figure 4.42: 3-D gain plot - Optimised antenna - 868 MHz

The 434 MHz case is interesting when looking at the resonance of the antenna structure, as can be seen in Figure 4.43. It resonates extremely well at 434 MHz, with a low bandwidth (and therefore a high Q). It does however seem if it will continue to resonate for frequencies from 450 MHz and upward, with an extremely large bandwidth, and low Q. The tuning components will determine the exact resonant frequency. This is not an ideal situation. For 868 MHz, the antenna has two resonant points close to each other (Figure 4.43). The exact resonating frequency of the antenna structure can be fine tuned by using tuning components close in value to the simulated 0.5 pF.

4.6 Theoretical Model Compared to Simulated Model

From the previous section, it can be seen that the theoretical model discussed in Section 4.2 compares well to the simulated results found. This is a good sign, as this indicates that the processed followed works. The next important step is to implement the simulated design and compare it to the simulated results, and thereby also compare it to the theoretical design.

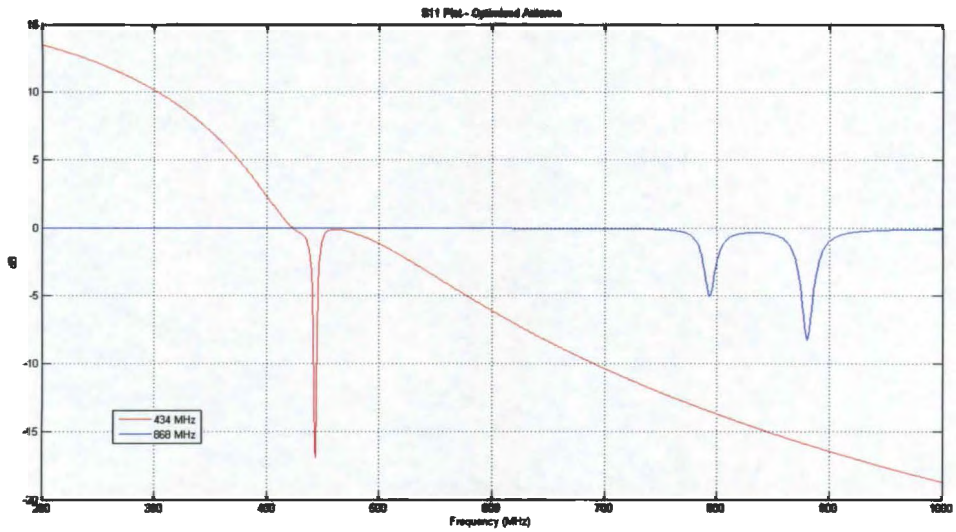

Figure 4.43: Comparison of S_{11} for 434 MHz and 868 MHz for the optimised antenna

4.7 Chapter review

Important aspects of the design of the antenna were discussed in this chapter. The theoretical design of the antenna was done where after various simulations were done and discussed. All of the simulations were variations of the original TCL antenna design. A preferred antenna design was chosen from the results obtained, where after it was optimised to ensure the best possible performance.

Chapter 5

Physical antenna implementation and results

The physical design of the antenna is discussed in this chapter. The characteristics of the antenna is also measured and discussed.

5.1 Introduction

The physical implementation of the antenna is discussed in this chapter. Together with the implementation of the antenna, the design of the transmitter circuit is discussed, since this is an important aspect when testing the new antenna design.

5.2 Design and construction

5.2.1 Enclosure and support structures

The design of the entire transmitter, including circuitry and antenna, is limited by the size of the enclosure. The enclosure is fitted around the ankle of the person being monitored and can therefore not be large. Figure 5.1 shows a concept drawing of a possible OID enclosure. The curve at the bottom of the enclosure is to ensure a tight fit around the curve of a human leg. This conceptual design measures $65mm \times 50mm \times 18mm$. This means the usable inside dimensions are $60mm \times 48mm \times 15mm$ and serves as the size constraint for the transmitter circuitry, antenna and battery.

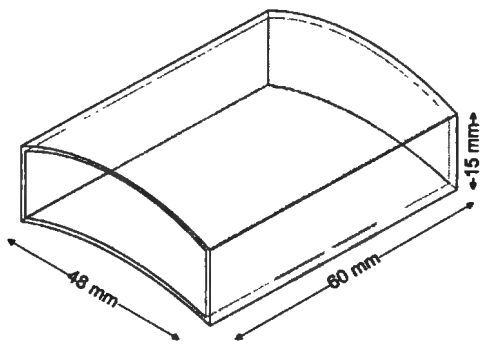

Figure 5.1: OID Enclosure Concept

5.2.2 PCB

From the above mentioned size constraints, the size of the PCB to be used can be taken as $60mm \times 48mm$ with a thickness of $1.6mm$. Although $1mm$ substrates are available, it is very brittle and not an ideal choice for this application. The $1.6mm$ substrate is more rigid and therefore allows for a more robust circuit. The antenna is partially etched onto the PCB and partially built above it. Since the PCB is inside the near-field region, it is safe to assume that it will influence the performance of the antenna. Ideally a high-frequency substrate material like Rogers Duroid should be used, but it is more

expensive than a material like FR4 laminate. For testing a new antenna design, the cost versus performance analysis is in favour of the FR4 laminate, even though it is not ideally suited for use in close proximity to a resonating structure. FR4 laminate was also used while simulating the antenna structure and a comparison between the simulated results and the actual results should be similar.

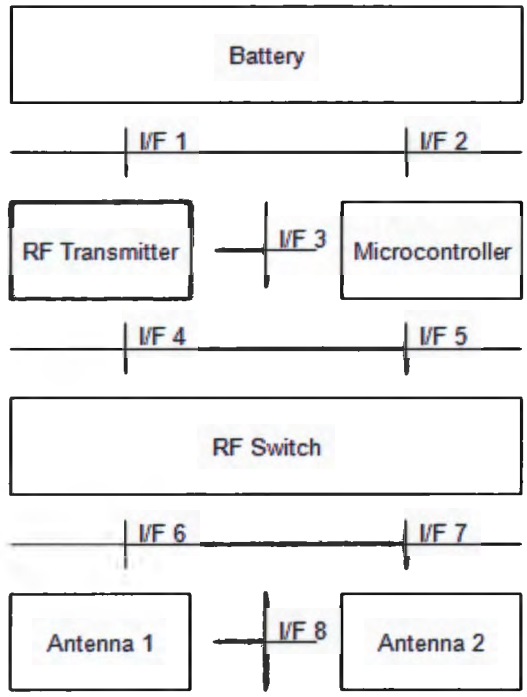

Figure 5.2: System diagram

Since the primary goal of this study is the development of an antenna, it was decided to use a commercial off-the-shelf transmitter, and not to design one. A transmitter module from Montar Manufacturing was selected, incorporating the Nordic Semiconductor nRF905 transceiver module. This transmitter has a 50Ω unbalanced output, for connecting an antenna with coaxial cable. The transmitter module requires input data to operate, which will be provided by a PIC12F microcontroller. All of this is shown in 5.2, with the interfaces indicated between the different parts of the system. Interface 1 and 2 is the connection of the battery to the RF transmitter and the microcontroller. Interface 3 is a Universal Asynchronous Receiver/Transmitter (UART) connection between the RF transmitter and the microcontroller. Interface 4 is a 50Ω coaxial feed to

the RF switch, while interface 5 is a connection between the microcontroller and the RF switch. This connection is responsible for switching between the two antennas.

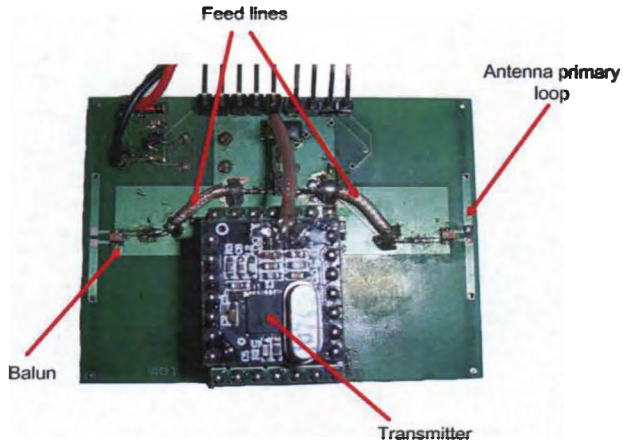

Figure 5.3: Bottom side of PCB

The transmitter, together with the feed lines, balun and primary loop are shown in Figure 5.3. The PIC12F1840 microcontroller, antenna structure and common primary-secondary loop is shown in Figure 5.4.

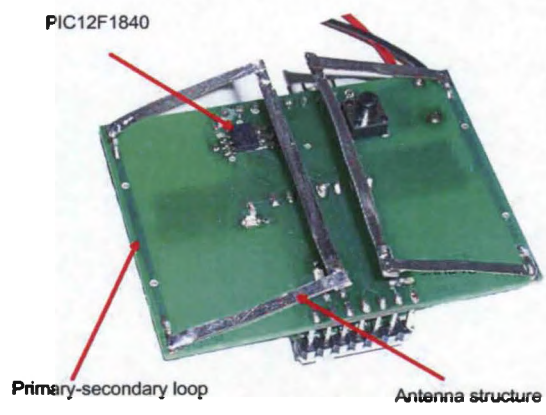

Figure 5.4: Top side of PCB

There are two antennas on the same PCB, with an RF switch selecting between the two antennas. Both of the antennas are clearly visible in Figure 5.4. The 50Ω output of the transmitter is connected to the RF switch with a low-loss 50Ω coaxial cable. The microcontroller controls the RF switch. The length of the feed lines leading to the

antennas is about $(\frac{1}{10})\lambda$ in length and it should therefore not be necessary to make these feed lines 50Ω. 50Ω feed lines are about 3 mm wide, therefore it also complicates the board layout for the rest of the circuit. A balun is used to convert the unbalanced feed line from the transmitter into a balanced feed on the primary loop of the antenna.

After implementing the design as described in the previous paragraph, it was seen that even though the feed lines are much shorter than a wavelength, it is still necessary to ensure that they are 50Ω. 50Ω coaxial cable was inserted between the RF switch and the baluns for both antennas.

The data to be transmitted will consist of a continuous string of binary $0's$ and $1's$. An example of this is 0101. The RF switch will switch between antennas after every binary value. Therefore all binary $1's$ will be transmitted by antenna 1, while antenna 2 will transmit the binary $0's$. This is illustrated in Figure 5.5. When looking at the signal received on the spectrum analyser, a distinction can be made between the signals received from the two antennas due to the Gaussian Frequency Shift Keying (GFSK) modulation scheme used by the transmitter.

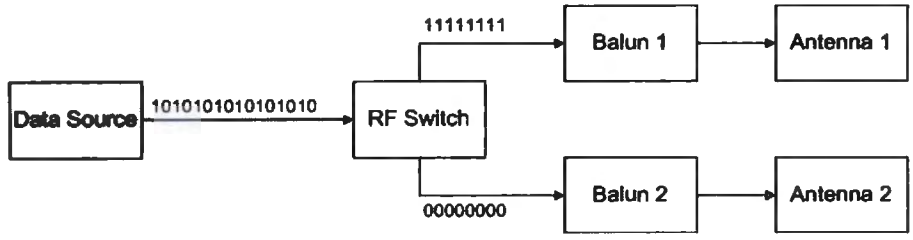

Figure 5.5: Illustration of data being transmitted

A matched receiver was not available for use and testing, and therefore the performance of the complete TCL antenna, which includes the transmission of data by both antennas, could not be tested in a real-world test set up.

Since a matched receiver for the transmitter was not used at the receiving end of the experiment, this part of the experiment was not used for testing, although it was implemented and fully functional.

5.2.3 Antenna structure

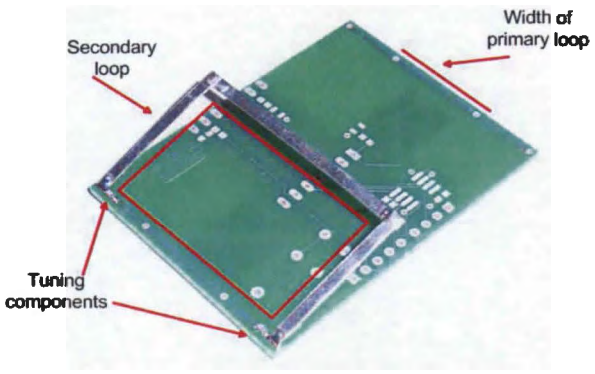

Figure 5.6: Empty PCB showing primary loop length and secondary loop

The primary loop of the antenna is etched onto the PCB. The side of the loop being fed is on the bottom of the PCB, with the mutual side with the secondary loop being on the top side of the PCB with vias connecting both sides of the loop with one another. The tuning components are located on the top track of the primary loop because it is difficult to mount a component on the three-dimensional structure. The metal structure of the antenna, forming the secondary loop, is made from a sheet of tin, as used in the simulation. This is soldered onto the track of the PCB, thereby forming the secondary loop. This structure is the maximum possible size, bounded by the OID enclosure. All of this is shown in Figure 5.6.

5.3 Experimental set up and test procedure

5.3.1 Experimental set up

Figure 5.7 is a schematic representation of the experimental set up. The characterisation of the antenna is of utmost importance and therefore the radiation pattern of the antenna must be measured in some way that is repeatable. To this end a table was made from polystyrene and PVC tubing (Figure 5.8). The synthetic materials used has a set dielectric constant, whereas with natural materials, like wood, the dielectric con-

stant varies according to the type of wood and its moisture content. The table has a rotating disc that is marked in 15° increments, ranging from -180° to 180°. A small cardboard box is used to separate the antenna under test from the table, to ensure that the table does not overly affect the antenna. The total height of this construction is 1.2 m.

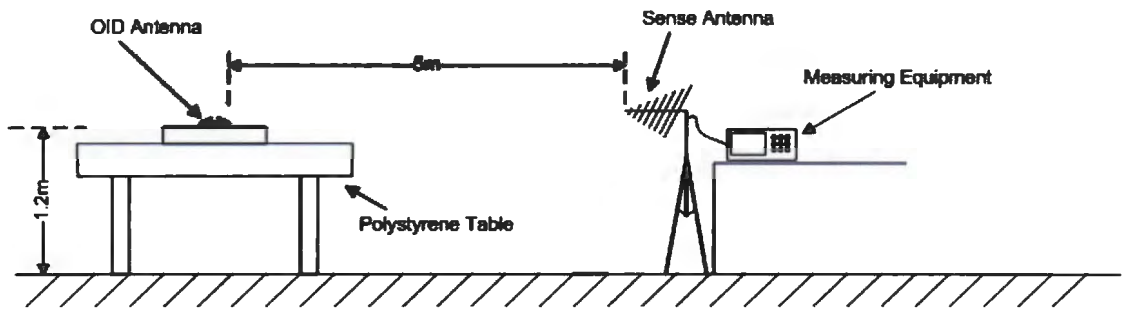

Figure 5.7: Experimental Set up

Figure 5.8: PVC and polystyrene table with rotating disc

A calibrated reception antenna is placed at the same height, on a camera tripod, pointing in the direction of the antenna being tested. This reception antenna is connected to a spectrum analyser. This set up is illustrated in Figure 5.9. The gain of this antenna is known to be 4 dBi, while the gain of the TCL antenna should be measured through this test.

The antenna being tested and the receiver antenna is placed 5 m apart to ensure that

Figure 5.9: Demonstration of receiving antenna connected to spectrum analyser

they are in the far-field regions of one another. Both antennas are placed as far as possible from any reflective surface, such as metal surfaces and strips found inside a building. To this end an empty parking area was used (Figure 5.10), where both the transmitter and receiver were placed approximately 20 m from the closest reflective surface. The building in the background of Figure 5.10 is at least 20 m from the experimental set up. Any reflections will need to travel at least 40 m before reaching the receiver, with a path loss of -83 dB at 434 MHz and -91 dB at 868 MHz, putting the reflections well beneath the measured noise floor.

Figure 5.10: Side view of experimental set up

5.3.2 Test procedure

Since space does not allow for the receiver antenna to be moved, this falls to the antenna being tested. It is placed horizontally on the rotating disc and an RF signal is fed to an antenna by the transmitter at the correct frequency, 434 MHz or 868 MHz. The spectrum analyser displays the amplitude of the received signal, which is then recorded. After each value has been recorded, the disc is rotated to the next azimuth angle and the received power level is again recorded. After a full rotation of the antenna, it is then elevated by a certain amount, in this case also in 15° increments ranging from -90° to 90°. These measurements will also allow for the calculation of the gain of the OID antenna.

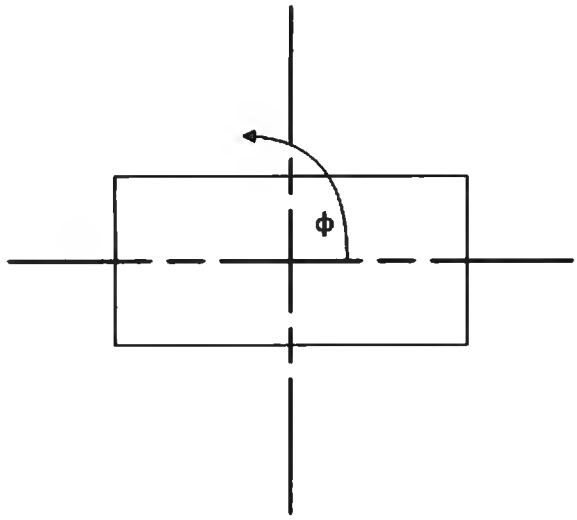

Figure 5.11: Azimuth Rotation, -180° $< \phi <$ 180°

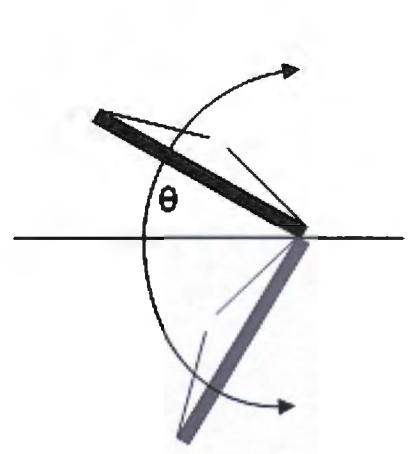

Figure 5.12: Elevation of Test Antenna, -90° $< \theta <$ 90°

5.4 Antenna measurements

The antenna was tested as discussed in the previous section. All of the results will be discussed to determine if the design of the TCL antenna meets the requirements set out in Chapter 1. It is also important to match the measured results with those obtained from the simulations. By doing this, the simulation results can be validated.

5.4.1 Free-space testing

The VSWR is a quantity that varies between 1 and ∞, where 1 indicates a matched load for the antenna. The transmitter used to test the antenna has a 50Ω output and therefore the impedance of the antenna should also be 50Ω. This should be the case for both 434 MHz and 868 MHz. The clearest way to illustrate this is by making use of a Smith chart in the form of$R + jX\Omega$. This is illustrated in Figure 5.13 (434 MHz) and Figure 5.14 (868 MHz). For 434 MHz, the marker indicates that the impedance of the antenna under test is $41.556\Omega + j27.866\Omega$. Thus, a small load mismatch exists between the transmitter and the antenna, which will result in a small loss. For 868 MHz, the impedance of the antenna is $56.826\Omega - j6.4145\Omega$, also resulting in a mismatched load, although it is closer to 50Ω. It should be taken into account that a lot of factors determine the impedance of the antenna and therefore an exact match is not likely with a product manufactured by hand.

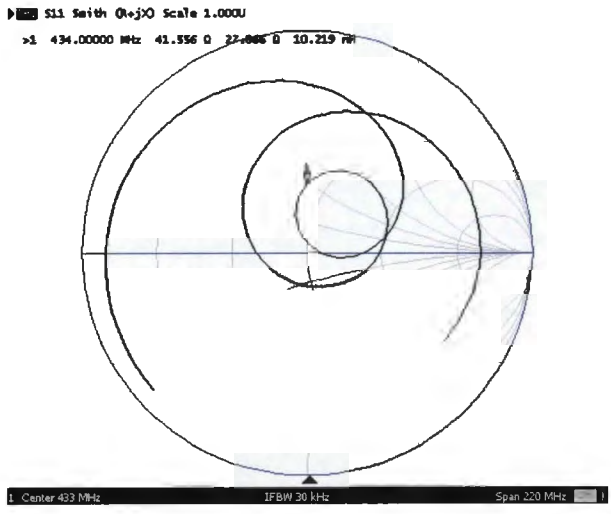

Figure 5.13: Smith Chart - 434 MHz

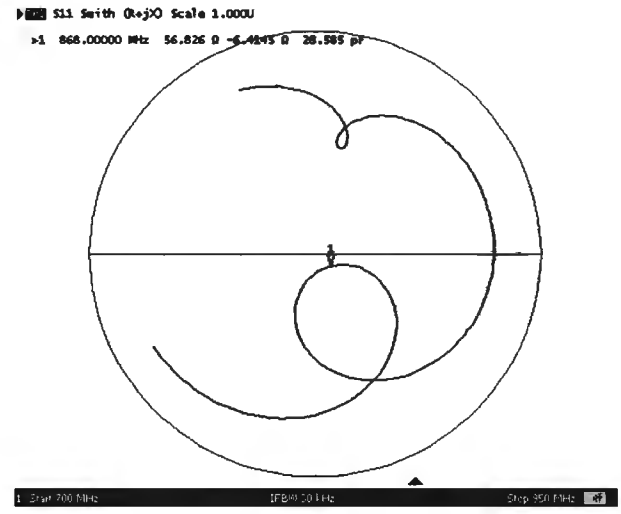

Figure 5.14: Smith Chart - 868 MHz

The S_{11} is shown on a log-magnitude plot for both frequencies. This will illustrate how well the antenna resonates. Figure 5.15 shows that at 434 MHz the antenna resonates well with the S_{11} value being -11.343 dB. The bandwidth of the antenna at the 3 dB

point is found to be 14.874 MHz.

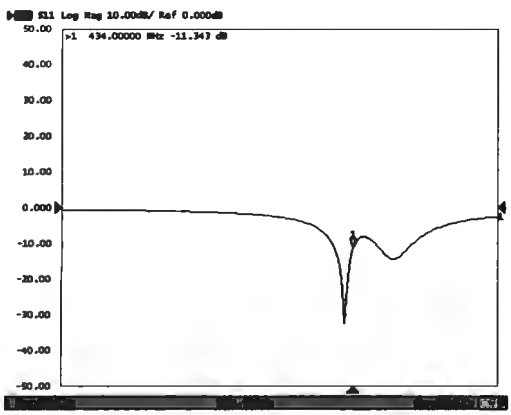

Figure 5.15: S_{11} for 434 MHz

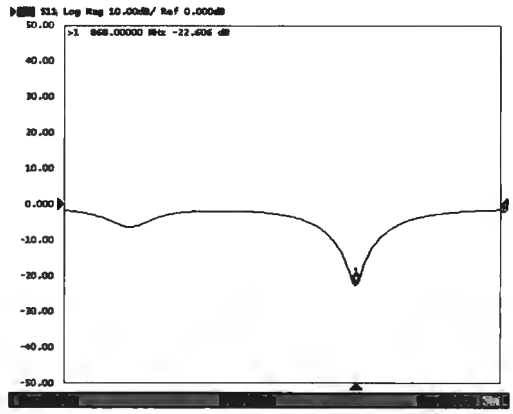

Figure 5.16: S_{11} for 868 MHz

Figure 5.16 shows that for 868 MHz the value of S_{11} is -22.606 dB which indicates that the antenna resonates extremely well. The bandwidth of the antenna at 868 MHz at the 3 dB point is 7.035 MHz.

Even though these results are by no means conclusive, it seems as if 868 MHz is the frequency to use, as its impedance is almost matched to the transmitter, it resonates well and has a higher Q than for 434 MHz.. This still needs to be confirmed with a test that includes a human analogue, as well as the measured radiation pattern.

5.4.2 Tests with human analogue

Figure 5.17 shows the impedance of the antenna at 434 MHz with a 1 litre saline solution placed beneath the antenna to act as a human analogue. The impedance of the antenna in close proximity to the human analogue is $91.24\Omega + j9.5044\Omega$, the real part being almost double that of the antenna without the human analogue. The saline solution therefore has a drastic effect on the impedance of the antenna. At 868 MHz the impedance of the antenna is $91.507\Omega - j19.435\Omega$, as shown in Figure 5.18. Without the saline solution, the impedance of the antenna at this frequency was close to 50Ω, thus

it has almost doubled.

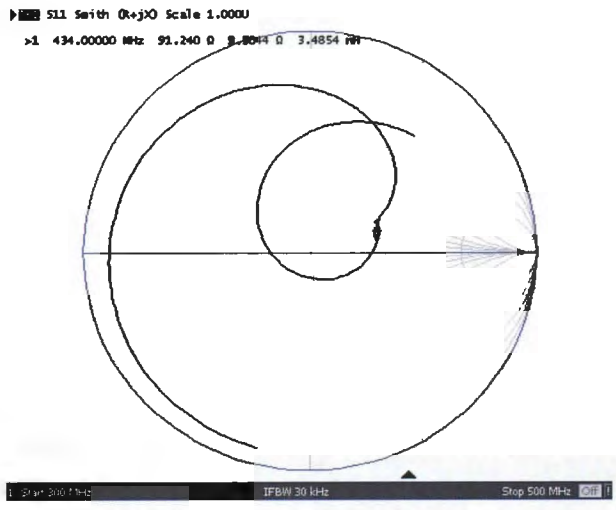

Figure 5.17: Smith Chart - 434 MHz - With Human Analogue

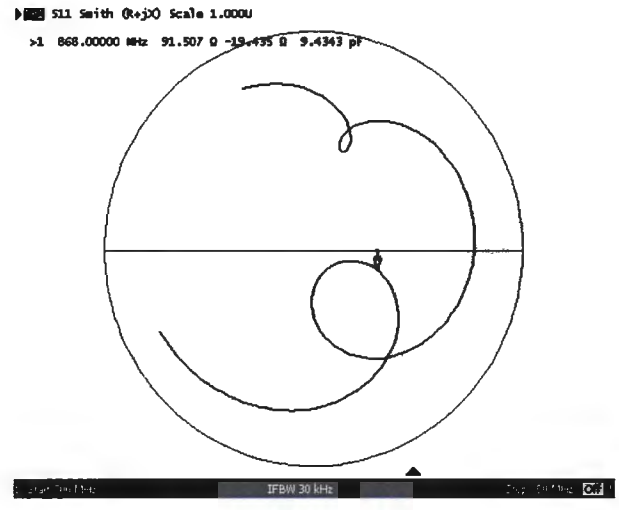

Figure 5.18: Smith Chart - 868 MHz - With Human Analogue

We now know that placing the antenna close to a human alters its impedance. Figure 5.19 shows that the antenna still resonates, albeit not quite as well, with the S_{11} value being -10.413 dB. The bandwidth at the 3 dB point has increased a lot however, being 61.908 MHz with the human analogue placed close to the antenna, about 4x the original bandwidth.

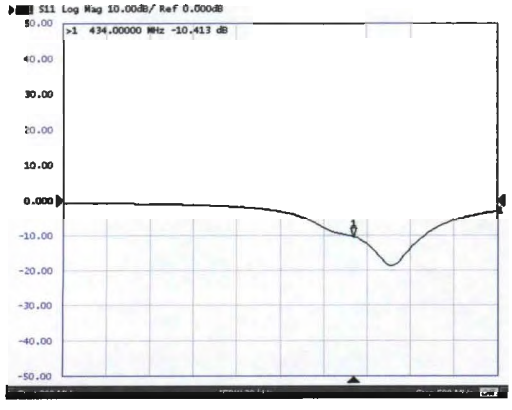

Figure 5.19: S_{11} for 434 MHz - With Human Analogue

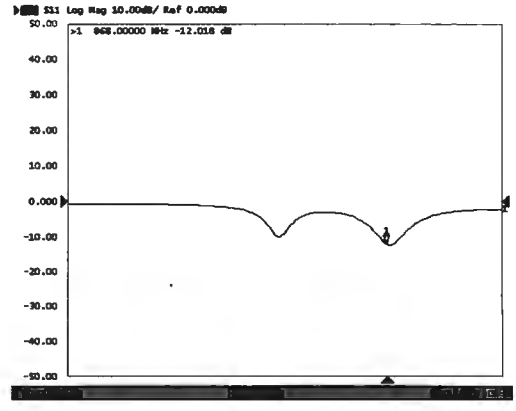

Figure 5.20: S_{11} for 868 MHz - With Human Analogue

At 868 MHz the S_{11} value is -12.018 dB, a difference of about 10 dB is thus experienced

when using the human analogue. The bandwidth of the antenna at the 3 dB point is 43.215 MHz compared to the previous bandwidth of 7.035 MHz, this is almost 6x wider.

5.4.3 Calculated path loss

The first step is calculating the free-space path loss, from Equation 5.1 [21].

$$L_{fs} = -27.55 + 20log_{10}fR \tag{5.1}$$

Equation 5.2 gives the general path loss experienced. C is the free-space path loss at 1 m, while n is a environmental factor. $n = 2$ gives a lossless model, while $n = 4$ is the loss in an dense urban environment [21].

$$PL = C + 10nlog_{10}R \tag{5.2}$$

The loss is a close enough approximation of the actual path loss in air and is therefore used. The free-space path loss is *39.18 dB* and *45.2 dB* over 5 m for 434 MHz and 868 MHz respectively. After the measurements are taken, the gain of the TCL antenna can then be calculated from these values.

This is not the total path loss of the antenna, since it does not take into account the transmitted power, gain of the transmitting and receiving antennas or insertion losses of components. Due to the mismatched impedance of the antenna when using the human analogue, an additional insertion loss exists that can be calculated as shown in Equation 5.3:

$$IL = -20log \mid 1 + \Gamma \mid = -20log \mid 1 + \frac{Z_{load} - 50}{Z_{load} - 50} \mid \tag{5.3}$$

Without the human analogue, the load mismatch is small, resulting in negligible insertion loss for both frequencies. When the human analogue is added, the load mismatch increases, resulting in an insertion loss of 5.1 dB for both frequencies. Additionally, the RF switch used has an insertion loss of 0.4 dB, while the balun has a maximum insertion loss of 1.9 dB. The path loss can then be calculated as follows:

$$TotalLoss = P_t + G_r - IL - PL \tag{5.4}$$

For 434 MHz in free-space, the loss is -29.11 dB, while it is -34.13 for 868 MHz. For 434 MHz when the human analogue is present, the loss is -34.22 dB and -39.23 dB at 868 MHz. This loss value should be added to the received power values to determine the gain of the antenna.

5.4.4 Radiation pattern

The radiation patterns for both frequencies will now be shown, with and without the human analogue. These results are then compared with the results obtained from the simulations. All results are available in Appendix A. For each configuration there are two radiation patterns. For the first one the elevation was kept at 0° and the azimuth was swept, while for the second radiation pattern discussed the azimuth was 0° and the elevation was swept. This should provide a good overview of the total radiation pattern of the antenna for both frequencies.

Figure 5.21 and Figure 5.22 shows the radiation pattern as measured compared to the radiation pattern obtained from the simulations, without a human analogue and with the human analogue respectively. The measured values shown indicates the gain of the antenna for the particular plane, after the path loss has been subtracted from the original measured values. For both situations the measured radiation pattern is similar, with a similar gain, to the the radiation pattern obtained from the simulations. There are several factors influencing the actual values. The environment used in the simula-

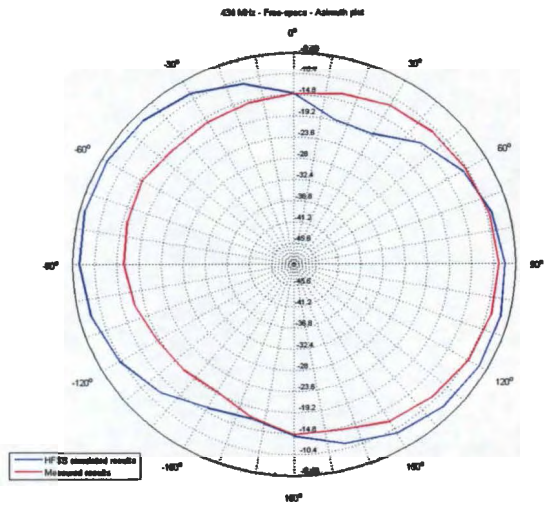

Figure 5.21: Radiation Pattern for 434 MHz - Elevation 0°

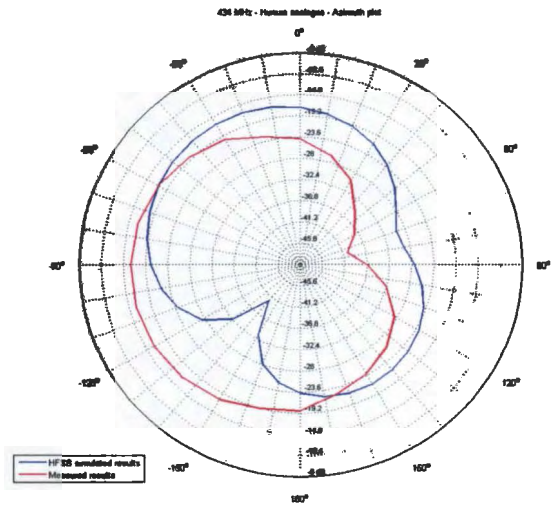

Figure 5.22: Radiation Pattern for 434 MHz - Elevation 0° - With Human Analogue

tion was perfect with no background noise or reflections from other sources interfering with the antenna measurements. A perfect environment is a physical impossibility and therefore it must be assumed that background noise exists as well as reflections from various sources in close proximity to the antenna being tested. The difference seen in Figure 5.21 between -30° and -120° and again at 30° can mainly be attributed to the implementation of the antenna. In Figure 5.22 it seems as if there exists an offset between the measured values and the simulated results. This is normal and can be expected when implementing an antenna. The simulated radiation pattern also is more directional compared to the measured results. The relatively omni-directional pattern seen in the measured results are preferable to the directional results.

Figure 5.23 shows the radiation pattern when the azimuth is 0°. The gain of the measured values are comparable to those from the simulation. The radiation pattern however does differ significantly from the simulation. Again the environment in which the antenna measurements were taken contributes to this. The resolution of the measurements also influences the pattern to a certain degree. If more measurements were taken, the radiation pattern measured might have been closer to the simulated radiation pattern, but it also takes more time.

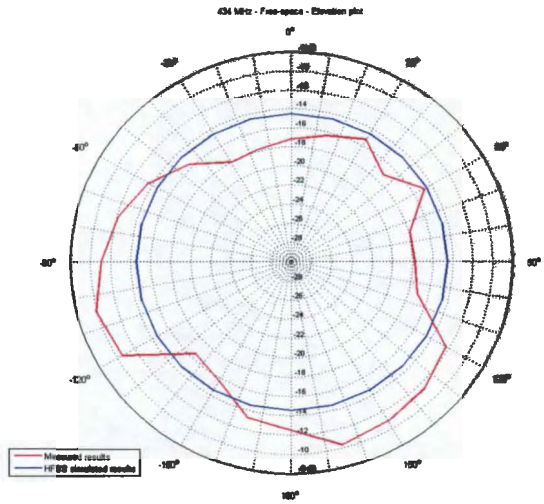

Figure 5.23: Radiation Pattern for 434 MHz - Azimuth 0°

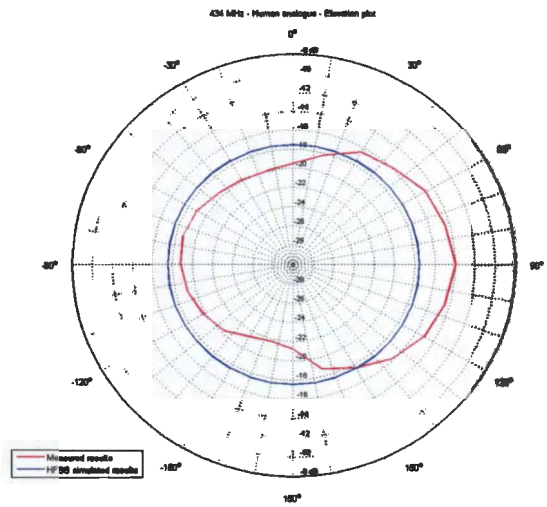

Figure 5.24: Radiation Pattern for 434 MHz - Azimuth 0° - With Human Analogue

Figure 5.25 shows the radiation pattern obtained when measuring the antenna at 868 MHz, compared to the simulation of the antenna for the same frequency. Again it can be said that the gain is similar to what is seen from the simulation, but the pattern is not an exact match. The biggest difference between the two results can be seen at 10° where the measured results shows a gain of -10 dB compared to the -29 dB of the simulated results. The resolution of the measurements, together with the environmental factors both contribute to this. Figure 5.26 shows the radiation pattern when the human analogue is used. The simulated antenna shows strong directionality , while the measured results are extremely omni-directional in this case.

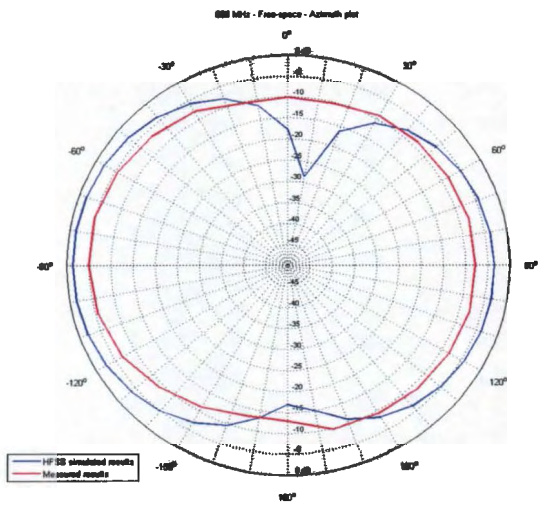

Figure 5.25: Radiation Pattern for 868 MHz - Elevation 0°

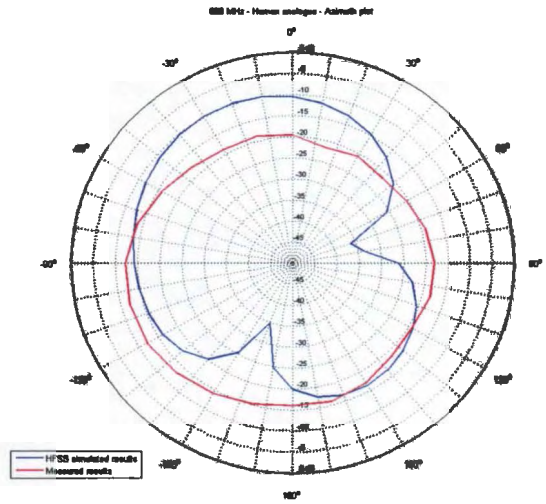

Figure 5.26: Radiation Pattern for 868 MHz - Elevation 0° - With Human Analogue

Figure 5.27 shows that the gain of the antenna when viewing it with an azimuth of 0° is similar to the simulation, but it differs at 0°, between 90° and -120°. The measured results in general tend to have less gain than the simulated results, especially in the above mentioned directions. Again the physical construction of the antenna is an important factor in explaining this difference. The ground plane will heavily influence this, especially in the 0° direction. Both the simulated results as well as the measured results are omni-directional when looking at the elevation plot, as seen in Figure 5.28. The difference between the two sets of results are very small, indicating that the human analogue reacts exactly as desired.

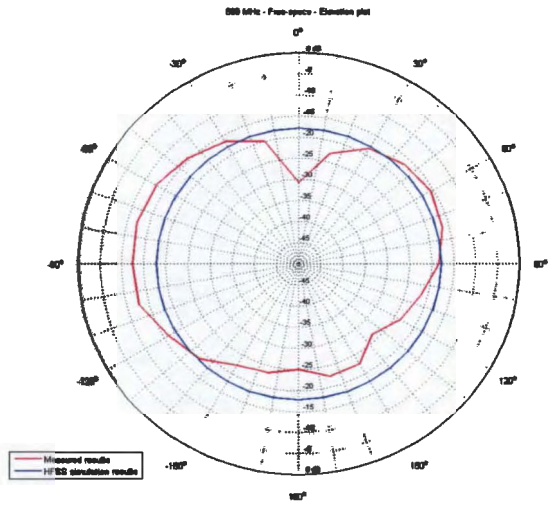

Figure 5.27: Radiation Pattern for 868 MHz - Azimuth 0°

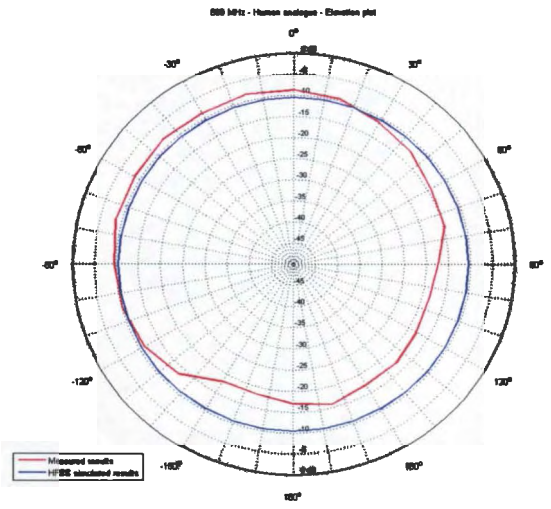

Figure 5.28: Radiation Pattern for 868 MHz - Azimuth 0° - With Human Analogue

5.4.5 Notes on the implementation

From the preceding sections, it could be seen that the implemented antenna performs similarly to the simulated antenna. This is the desired result and therefore expected, if the antenna is implemented as close as possible to the simulated antenna. However, there are some issues that need to be addressed.

- **Implementation** The simulated antenna doesn't take into account the exact implementation. The biggest factor influencing the antenna performance after implementation is a relatively large ground plane, compared to the size of the substrate used. The ground plane is necessary for the electronics that implements the OID and the test platform. The plug-in module used for the transmitter also negatively impacts performance, as it places another large piece of FR4 epoxy substrate in the reactive near-field of the antenna. The antenna matching should also be done when placing the antenna close to the human analogue. This will ensure correct operation with good overall performance if the OID should be implemented.

- **Construction** Under ideal circumstances, the antenna structure should be laser-cut, to ensure that it matches the antenna used in the simulation. This will also

eliminate any manufacturing errors made during the construction phase of this project where the antennas were cut and soldered by hand, since the effect of this is unknown;

- **Test Environment** Ideally the antenna must be characterised in an anechoic chamber or a characterised open-field environment. These tests are expensive and unnecessary if a proof-of-concept is all that is required. If the correct transmitter, as used in an OID, could be used together with the correct enclosure and battery, the characterisation tests can be even more accurate, since there are no reflections or the reflections are known.

5.5 Chapter Review

This chapter discussed several aspects relating to the physical realisation of the antenna and test set up. After a brief explanation of the test set up and procedures a selection of test results were presented. Any variation between measured data and simulated predictions are then explained and justified. In general a good correlation exists between measured and simulated results. The main deviations can be attributed to environmental factors together with construction effects.

Chapter 6

Conclusion and recommendations

In this chapter conclusions are drawn regarding the design, manufacturing and operational success of the antenna. Recommendations are also made for possible future work.

6.1 Conclusion

6.1.1 Research objectives

Even with the noted deviation from the simulated results, the antenna performed reasonably well. The main research objective, of designing a small antenna for indoor electronic monitoring within certain constraints, was thus achieved. With regards to the secondary research objectives, it was found that most wireless communication protocols are not suitable for this application, and therefore a proprietary communication technology should result in the best possible performance of the system. When looking at the results in Section 5.4, it can be seen that the impedance of the antenna structure was matched quite easily to 50Ω at 868 MHz, but at 434 MHz this was not so easy. The antenna structure also resonates better at 868 MHz.

6.1.2 Design process

In Section 3.2 the complete antenna design process was to be followed was discussed in-depth. The various stages of this design process was followed and proved to be a viable design methodology for the design of an antenna. One of the main reasons for the success of this design methodology was that the requirements for the antenna was specified very early on together with all of the constraints placed on the antenna.

6.1.3 Simulation of antenna structures

By first doing preliminary simulations, early antenna prototypes could be eliminated before too much resources were spent on them, leaving all of the available resources to be consumed by antenna structures that showed potential. Additional antenna structures are available in Appendix A. A lot of time was spent on the detailed simulation of the antenna structures addressed in Section 4.4 to investigate the effect of structural changes on the effectiveness of the TCL antenna. The choice of structures was eventually limited to five antenna structures, of which the best possible one was chosen when comparing certain antenna parameters. It was this antenna structure that was manufactured, due to its simulated performance.

6.1.4 Measured antenna performance

In Section 5.2 the physical implementation of the antenna and test-platform was discussed. It is important to note the differences between the simulated antenna and the physical antenna structure. When simulating an antenna structure, the physical environment is not taken into account. This is especially true for the propagation effects discussed in Section 2.3.2. The simulated environment assumes that the antenna is in free-space. Since this antenna design is used as a proof-of-concept, it is not necessary to test the antenna in a characterised environment, or an anechoic chamber. This is especially true since it is also resource-intensive to professionally characterise an antenna.

The open-space environment is sufficiently free of any possible source of reflections. The surrounding environment thus has less of an influence on antenna performance. The deviation of measured results from the simulations can mostly be attributed to the construction of the physical antenna structure and the associated transmitter module.

The tests performed in the outdoor environment does not accurately predict the operation of the OID in a real-world environment, since the OID will not exclusively be used in an outdoor environment, but in an indoor environment as well. The materials used in the construction of buildings cause reflections that may interfere with the operation of the OID. The most obvious result is that the range of the transmitter is limited when used indoors. This should be considered when implementing the OID.

6.2 Recommendations

For possible future work on this project, including improvements on the current design, there are a few recommendations to be made:

1. Simulation
    - When simulating the antenna structure, be as accurate as possible. The inclusion of possible ground and other power planes on the substrate is very important, resulting in a higher correlation between measured and simulated results;
2. Physical implementation
    - The correct transmitter must be used. This is the transmitter earmarked for use in the OID. The use of the correct transmitter will minimise the possible effect the current transmitter plug-in module has on the performance of the antenna. Modern embedded transmitter modules can be found as part of a System-on-Chip (SoC), enabling the substrate to make do with a relatively

small ground and power plane. A SoC can also be placed directly on the PCB and not as a plug-in module;

3. Measurement set up

   - RF feed lines should have the correct impedance, dependent on the substrate material, -thickness and the frequency;
   - All components, including the matching network, should be placed on the PCB in a repeatable way, such as with a reflow oven. This will minimise mistakes made during hand-soldering of the components;
   - The antenna structure should ideally be laser-cut from metal sheets;
   - The correct OID enclosure and strap should be available for use during the simulation and testing phase of the antenna. This will increase the accuracy of any measurements taken, and proper range testing can then also be conducted;

4. Performance testing

   - The characterisation of the antenna should preferably be done in an open-field or other characterised environment. Such services can be rendered by professionals;
   - By using a receiver matched to the transmitter, data can be sent from the transmitter to the receiver, after which the integrity of the received data can be verified. This is not possible when looking at the received signal on a spectrum analyser. By doing this, the combined performance of both antennas used in an OID can be measured.

Bibliography

[1] N. Mapisa-Nqakula, *Annual Report for the 2010/2011 Financial Year*. Department: Correctional Services, 2011.

[2] R. Gable, "Application of personal telemonitoring to current problems in corrections," *Journal of Criminal Justice*, vol. 14, no. 2, pp. 167–176, 1986.

[3] R. Blake, *Wireless Communication Technology*, 1st ed., S. Clark, Ed. Delmar Thompson Learning, 2001.

[4] L. Frenzel, *Priciples of Electronic Communication Systems*, T. Casson, Ed. McGraw-Hill, 2008.

[5] L. Ahlin, *Principles of Wireless Communications*. Professional Publishing Svc, 2006.

[6] N. Maslin, *HF Communications: A Systems Approach*. Pitman, 1987.

[7] W. Boddy, *Fifties Television: The Industry and its Critics*. University of Illinois Press, 1993.

[8] (2011, September) Definitions of ISM bands. Website. International Telecommunication Union. [Online]. Available: http://www.itu.int/ITU-R/terrestrial/faq/index.html#g013

[9] J. C. Maxwell, "A dynamical theory of the electromagnetic field," *Royal Society of London Philosophical Transactions Series I*, vol. 155, pp. 459–512, 1865.

[10] W. Stutzman and G. Thiele, *Antenna Theory and Design*, 2nd ed. John Wiley and Sons, 1998.

[11] K. Kishore, *Antenna and Wave Propagation*, 1st ed. I.K. International Publishing House Pvt. Ltd., 2009.

[12] D. Pozar, *Microwave Engineering*, 3rd ed., B. Zobrist, Ed. John Wiley and Sons, 2005.

[13] J. White, *High Frequency Techniques - An Introduction to RF and Microwave Engineering*. Wiley-IEEE Press, 2004.

[14] J. Walfisch, "A theoretical model of uhf propagation in urban environments," *IEEE Transactions on An*, vol. 36, no. 12, pp. 1788–1796, December 1988.

[15] H. Friis, "A note on a simple transmission formula," *Procedings of the IRE*, vol. 34, pp. 254–256, 1946.

[16] J. Proakis, *Digital Communications*. McGraw-Hill, 1995.

[17] J. Ling, D. Chizhik, P. Wolniansky, R. Valenzuela, N. Costa, and K. Huber, "Multiple transmit multiple receive (MTMR) capacity survey in manhattan," *Electronics Letters*, vol. 37, no. 16, pp. 1041–1042, August 2001.

[18] M. Simon and M. Alouini, *Digital Comm Over Fading Channels*. John Wiley and Sons, 2005.

[19] D. Tse and P. Viswanath, *Fundamentals of Wireless Communication*. Cambridge University Press, 2005.

[20] M. Hata, "Empirical formula for propagation loss in land mobile radio services," *IEEE Transactions on Vehical Technology*, vol. 29, no. 3, pp. 317–325, August 1980.

[21] L. van Loon, "Mobile in-home UHF radio propagation for short-range devices," *IEEE Antennas and Wirelss Propagation Magazine*, vol. 41, no. 2, pp. 37–40, April 1999.

[22] H. Marais, "Characterization of an UHF fading channel for an RFID-based EVI system," Master's thesis, North-West University, 2009.

[23] T. Milligan, *Modern Antenna Design*. John Wiley and Sons, 2005.

[24] C. Balanis, *Antenna Theory: Analysis and Design*, 2nd ed. John Wiley and Sons, 1997.

[25] K. Fujimoto, A. Henderson, K. Hirasawa, and J. James, *Small Antennas*, J. James, Ed. Research Studies Press, 1987.

[26] J. van Niekerk, "Matching small loop antennas to rfPIC devices," Microchip Technology Inc., Tech. Rep., 2002.

[27] B. SIG. Bluetooth special interest group. Website. Bluetooth SIG. [Online]. Available: http://www.bluetooth.org

[28] W.-F. Alliance. (2011, September) Wi-fi alliance homepage. Website. Wi-Fi Alliance. [Online]. Available: http://www.wi-fi.org

[29] W. Dargie, *Fundamentals of Wireless Sensor Networks: Theory and Practice.* John Wiley and Sons, 2010.

[30] K. Sohraby, *Wireless Sensor Networks: Technology, Protocols and Applications.* Wiley-Interscience, 2007.

[31] P. Kinney, "Zigbee technology: Wireless control that simply works," IEEE 802.15.4 Task Group, Tech. Rep., October 2003.

[32] D. Gustafsson, "WirelessHART-implementation and evaluation on wireless sensors," Master's thesis, KTH Electrical Engineering, 2009.

[33] R. Harrington, *Field Computation by Moment Methods.* IEEE Press, 1993.

[34] P. Lounesto, *Clifford Algebras and Spinors.* Cambridge University Press, 1997.

[35] A. Taflove, *Computational Electrodynamics: The Finite-Difference Time-Domain Method.* Artech House, 2005.

[36] J. Jin, *The Finite Element Method in Electromagnetics*, 2nd ed. John Wiley and Sons, 2002.

[37] M. Sadiku, *Numerical Techniques in Electromagnetics.* CRC Press, 2000.

[38] A. Corporation. (2011, July) Ansoft high frequency structure simulator. Website. Ansoft Corporation. [Online]. Available: http://www.ansoft.com

Appendix A

Appendix

A.1 Simulation Results

All results are supplied in digital format (.hfss). Any PC with Ansoft HFSS 13 or higher can run the simulation file to generate the results.

A.2 Measured Results

The measured results are supplied in digital format (.xlsx).

A.3 Pictures and Photo's

All figures, including photo's used in the dissertation are included on the disc.

A.4 Other

A digital copy of the dissertation (.pdf) is also included on the disc.